

ROBUST CROSSFEED DESIGN FOR  
HOVERING ROTORCRAFT

*NCC 2-751*

A Thesis Presented to the Faculty of  
California Polytechnic State University  
San Luis Obispo

In Partial Fulfillment  
of the Requirements for the Degree of  
Master of Science in Aeronautical Engineering

by  
David R. Catapang

April 1993

*GRANT  
IN-05-CR  
167281*

*p-70*

N93-27241

Unclas

G3/05 0167281

(NASA-CR-193107) ROBUST CROSSFEED  
DESIGN FOR HOVERING ROTORCRAFT M.S.  
Thesis (California Polytechnic  
State Univ.) 70 p

AUTHORIZATION FOR REPRODUCTION  
OF MASTER'S THESIS

I grant permission for the reproduction of this thesis in its entirety or any of its parts,  
without further authorization from me.

David Catering  
Signature

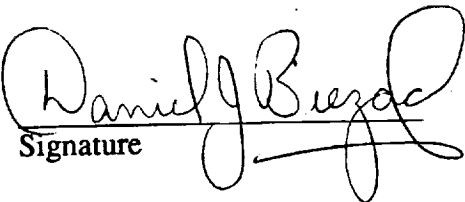
April 20, 1993

Date

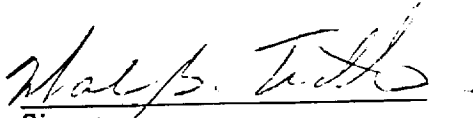
## APPROVAL PAGE

TITLE: Robust Crossfeed Design for Hovering Rotorcraft  
AUTHOR: David R. Catapang  
DATE SUBMITTED: April 1993


Daniel J. Biezad  
Thesis Advisor  
Aeronautical Engineering  
Cal Poly, San Luis Obispo

  
Signature

Mark B. Tischler  
Committee Member / Research Sponsor  
U. S. Army Aeroflightdynamics Directorate  
Ames Research Center, Moffett Field

  
Signature

Jin Tso  
Committee Member  
Aeronautical Engineering  
Cal Poly, San Luis Obispo

  
Signature

Carl A. MacCarley  
Committee Member  
Electronic / Electrical Engineering  
Cal Poly, San Luis Obispo

  
Signature

**ABSTRACT**  
**ROBUST CROSSFEED DESIGN FOR HOVERING ROTORCRAFT**

**David R. Catapang**

**April 1993**

Control law design for rotorcraft fly-by-wire systems normally attempts to decouple angular responses using fixed-gain crossfeeds. This approach can lead to poor decoupling over the frequency range of pilot inputs and increase the load on the feedback loops. In order to improve the decoupling performance, dynamic crossfeeds may be adopted. Moreover, because of the large changes that occur in rotorcraft dynamics due to small changes about the nominal design condition, especially for near-hovering flight, the crossfeed design must be "robust." A new low-order matching method is presented here to design robust crossfeed compensators for multi-input, multi-output (MIMO) systems. The technique identifies degrees-of-freedom that can be decoupled using crossfeeds, given an anticipated set of parameter variations for the range of flight conditions of concern. Cross-coupling is then reduced for degrees-of-freedom that can use crossfeed compensation by minimizing off-axis response magnitude average and variance. Results are presented for the analysis of pitch, roll, yaw and heave coupling of the UH-60 Black Hawk helicopter in near-hovering flight. Robust crossfeeds are designed that show significant improvement in decoupling performance and robustness over nominal, single design point, compensators. The design method and results are presented in an easily-used graphical format that lends significant physical insight to the design procedure. This plant pre-compensation technique is an appropriate preliminary step to the design of robust feedback control laws for rotorcraft.

## ACKNOWLEDGMENTS

This research was funded by NASA Grant NCC 2-751. I am grateful for the support and facilities of the Flight Dynamics and Controls Branch for accomplishing my work. Special thanks to Dr. Mark Tischler for his guidance and insight which gave me great appreciation for the research process.

I would also like to thank the faculty of Cal Poly, San Luis Obispo for their tradition of quality engineering education, which allowed me to experience a great spectrum of possible career opportunities in between the years of classes. I especially am grateful to Dr. Daniel Biezdad for his experience and enthusiasm in research work which inspired me to find the same spirit in myself.

I dedicate this research to my parents, Arthur and Estelita Catapang, who have so patiently supported my education and exploration for a worthwhile and meaningful career.

## TABLE OF CONTENTS

CHAPTER I. INTRODUCTION.....	1
<i>Background</i> .....	1
<i>Purpose</i> .....	2
<i>Scope</i> .....	2
<i>Organization</i> .....	3
CHAPTER II. LITERATURE REVIEW.....	4
<i>Coupling Numerator Theory</i> .....	4
<i>Quantitative Feedback Theory</i> .....	5
<i>Previous Related Work</i> .....	6
CHAPTER III. RESEARCH PROCEDURE.....	7
<i>Modeling of the Rotorcraft and Control System</i> .....	7
<u>Illustration of the 2x2 decoupling problem</u> .....	7
<u>Explanation of the 4x4 decoupling problem</u> .....	8
<u>The rotorcraft mathematical model</u> .....	9
<u>Variation of flight conditions</u> .....	10
<i>Uncompensated Response and Ideal Crossfeeds for the 4 x 4 Case</i> .....	10
<u>Frequency range of interest for heave and rate responses</u> .....	10
<u>Compensated response</u> .....	11
<u>Ideal crossfeed calculation for the 4 x 4 system</u> .....	13

<i>Low-Order Approximation of the Ideal Crossfeeds</i> .....	14
<u>Characteristics of the ideal crossfeed</u> .....	14
<u>Low-order crossfeed fit to a nominal ideal crossfeed</u> .....	15
<i>Decoupling Performance Metric</i> .....	16
<u>Evaluation of robust decoupling for a set</u> .....	16
<u>of flight conditions</u>	
<u>Consideration of coupling variance</u> .....	17
<i>Graphical Basis for Robust Crossfeed Design</i> .....	17
<i>The Mean Square Weighting (MSW) Strategy</i> .....	20
<u>Target crossfeeds</u> .....	20
<u>Frequency weighting</u> .....	22
<i>Template Analysis</i> .....	23
<u>Influential points</u> .....	23
<u>Robust regression and outlier detection</u> .....	23
<u>Condition for existence of a practical low-order crossfeed</u> ....	23
<u>Template analysis results for the 4x4 case</u> .....	24
<b>CHAPTER IV. ANALYSIS OF RESULTS</b> .....	30
<i>Crossfeed Compensation Summary</i> .....	30
<i>Performance Improvement Summary</i> .....	31
<i>Scatter Plots</i> .....	32
<i>Bode Plots</i> .....	35
<i>Time Response Plots</i> .....	38

<b>CHAPTER V. CONCLUSIONS.....</b>	<b>43</b>
<b>REFERENCES.....</b>	<b>45</b>
<b>APPENDIX A. DERIVATION OF COUPLING NUMERATORS .....</b>	<b>48</b>
<b>FOR PITCH-ROLL COUPLING</b>	
<b>APPENDIX B. CONFIGURATION MATRICES.....</b>	<b>52</b>



## LIST OF TABLES

Table I - Variation of Configurations.....	10
Table II - Lateral Cyclic Input Responses.....	11
Table III - Longitudinal Cyclic Input Responses.....	11
Table IV - Tail Rotor Collective Input Responses.....	12
Table V - Main Rotor Collective Input Responses.....	12
Table VI - Approximations to the Ideal Crossfeeds.....	14
for the Nominal Configuration	
Table VII - Sample Target Crossfeed Values.....	22
Table VIII - Features of the Crossfeed Templates.....	24
Table IX - Configuration Influence for $G_{\delta_c}^{\delta_a}$ .....	25
Table X - Configuration Influence for $G_{\delta_c}^{\delta_r}$ .....	26
Table XI - Configuration Influence for $G_{\delta_c}^{\delta_r}$ .....	26
Table XII - Average Metrics.....	30
Table XIII - Summary of MSW Crossfeeds.....	31
Table XIV - Compensated Off-Axis Metrics.....	31
Table XV - Bode Plot Features.....	33
Table XVI - Representative Time Response for Roll/Pitch Coupling.....	39
Table XVII - Representative Time Response for Yaw/Heave Coupling.....	39

## LIST OF FIGURES

Figure 1 - RASCAL UH-60 Black Hawk.....	2
Figure 2 - QFT Design on the Nichols Plot.....	6
Figure 3 - Control System Block Diagram.....	8
Figure 4 - Crossfeeds for the 4x4 System.....	9
Figure 5 - Low Order Fit to Ideal Crossfeed.....	15
Figure 6 - Nichols Chart Representation of Low-Order Approximation.....	18
Figure 7- Frequency Templates of Ideal Crossfeeds.....	19
Figure 8 - MSW Strategy with Synthesized Templates.....	21
Figure 9 - Templates of Influential Crossfeed Points for $G_{\delta_c}^{\delta_r}$ .....	27
Figure 10 - Templates of Influential Crossfeed Points for $G_{\delta_r}^{\delta_c}$ .....	28
Figure 11 - Templates of Influential Crossfeed Points for $G_{\delta_c}^{\delta_r}$ .....	29
Figure 12 - Comparison of Decoupling Averages for $p / \delta_e$ .....	33
Figure 13 - Comparison of Decoupling Averages for $r / \delta_c$ .....	34
Figure 14 - Nominal vs . Uncompensated Metric Bode Plot: $p / \delta_e$ .....	37
Figure 15 - Nominal vs. MSW Metric Bode Plot: $p / \delta_e$ .....	37
Figure 16 - Nominal vs . Uncompensated Metric Bode Plot: $r / \delta_c$ .....	38
Figure 17 - Nominal vs. MSW Metric Bode Plot: $r / \delta_c$ .....	38
Figure 18 - Uncompensated Time Response: Roll / Pitch.....	40
Figure 19 - Uncompensated Time Response: Yaw / Heave.....	40
Figure 20 - Nominal Time Response: Roll / Pitch.....	41
Figure 21 - Nominal Time Response: Yaw / Heave.....	41
Figure 22 - MSW Time Response: Roll / Pitch.....	42
Figure 23 - MSW Time Response: Yaw / Heave.....	42
Figure 24 - State Space Diagram of the 2x2 Decoupling Problem.....	49

## NOMENCLATURE

<b>A</b>	State matrix
<b>B</b>	Control matrix
$F_x$	Forward compensation for "x" degree of freedom
$G_x$	Feedback compensation for "x" degree of freedom
$G_{\delta_x}^{\delta_y}(\#1_{LO})$	Low-order crossfeed fit to nominal ideal crossfeed that channels "x" command into "y" input to the plant.
$J_{avg}$	Average decoupling metric (dB)
$J_{\sigma}$	Cost of variance (dB)
$J_{total}$	Robust decoupling metric (dB)
<b>N</b>	Determinant of numerator matrix
$N_{\delta_a \delta_r}^{q r}$	Coupling numerator
<b>MIMO</b>	Multiple-Input, Multiple-Output
<b>MSW</b>	Mean Square Weighting
<b>P</b>	Square matrix of coupling numerators for generating ideal crossfeeds
<b>QFT</b>	Quantitative Feedback Theory
<b>RASCAL</b>	Rotorcraft Aircrew Systems and Controls Airborne Laboratory
<b>m</b>	Total number of frequencies used within frequency range of interest
$\overline{\mathbf{m}}$	Vector of ideal crossfeeds
<b>n</b>	Total number of configurations that are being analyzed
<b>p</b>	Roll rate (rad/sec)

$q$	Pitch rate (rad/sec)
$r$	Yaw rate (rad/sec)
$s$	Laplace transform
$\bar{u}$	Control vector
$w$	Heave [vertical velocity] (ft/sec)
$w_{msw,i,j}$	Mean square weight for frequency "i" at configuration "j"
$w_j$	Configuration weight related to group of likelihood
$w_{NAVFIT,i}$	NAVFIT weight for frequency "i"
$\bar{x}$	State vector
$\bar{y}$	Vector of coupling numerators for generating ideal crossfeeds
$\Delta M_j$	Average decoupling of one configuration over m frequencies
$\Phi$	Roll Angle (rad)
$\Theta$	Pitch Angle (rad)
$\delta_a$	Lateral cyclic (in.)
$\delta_c$	Longitudinal cyclic (in.)
$\delta_r$	Tail collective (in.)
$\delta_c$	Main collective (in.)

## CHAPTER I

### INTRODUCTION

Cross-coupling in near-hover conditions is a characteristic problem for helicopter flight control system design. Cross-coupling occurs when an off-axis response occurs as a result of an on-axis command. An example of cross-coupling is roll rate due to pitch command. Cross-coupling is frequency dependent and can be modeled with transfer functions through linearization of flight dynamics. This allows cross-coupling to be reduced with a flight control system designed using classical control theory.

#### ***Background***

The UH-60 Black Hawk (fig. 1) is representative of a helicopter with highly coupled motion in hover because of its single main rotor and canted tail rotor that is located above the center of gravity. The Black Hawk will be used as the Rotorcraft Aircrew Systems and Controls Airborne Laboratory (RASCAL), a joint U. S. Army / NASA program to evaluate advanced controls and systems concepts (ref. 1). A key goal of the flight control design for RASCAL is to achieve high bandwidth and decoupled response characteristics as required by the current helicopter handling qualities specification (ref. 2). The requirements must be met under various flight conditions such as different wind directions and speeds, rotorcraft weight and center of gravity location, and ascending or descending flight.

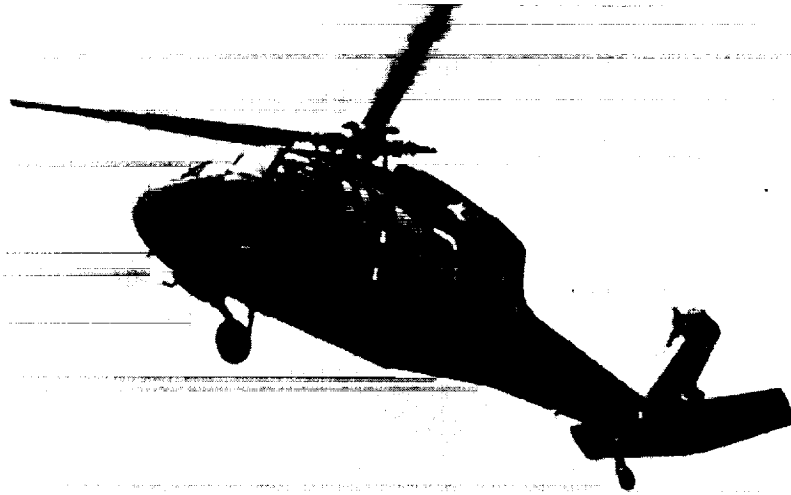


**Figure 1 - RASCAL UH-60 Black Hawk**

### ***Purpose***

The focus of this study is the decoupling aspect of the flight control system. Cross-coupling characteristics are expected to vary greatly with flight condition. Therefore the main purpose of this study is to achieve acceptable decoupling characteristics in hovering flight despite variation of flight dynamics. Desired decoupling characteristics will be shown to be off-axis response reduced from bare airframe levels with minimal variation for a set of flight conditions.

### ***Scope***

This study addresses three main aspects of multi-input, multi-output (MIMO) flight control system design; system architecture, decoupling, and robustness. System architecture deals with the issue of whether decoupling should be achieved by feedback or by crossfeeds. Decoupling can be achieved through the use of high gains on the feedback loop. High feedback gains also add robustness to a system against plant variation. Adverse effects of high feedback gain were reported in ref. 3 as control limiting and closed-loop instability.

Crossfeeds are an open-loop control strategy that may minimize the use of feedback gain. Crossfeeds involve command input into two channels of the controlled element on-axis and off-axis inputs with the result that the off-axis input to off-axis output will cancel the response of on-axis input to off-axis output. This is accomplished by multiplying the initial on-axis input by a crossfeed to generate the canceling off-axis output, which can be a gain or a low-order transfer function. This open-loop control strategy is sensitive to flight condition variation because one crossfeed will completely cancel off-axis response for a certain flight condition. Crossfeed compensation may not be robust if variation in flight conditions are large or unknown. However this study presumes that the variation of flight conditions is limited and known. Therefore a robust crossfeed flight control design can be accomplished through analysis of helicopter flight dynamics for several variations of near-hover conditions.

### ***Organization***

The evolution of this study is described in the following chapters. Chapter II is a review of literature containing theory and methods of presentation of data related to this study. Highlights of Chapter II are coupling numerator theory, quantitative feedback theory, and a preliminary study of robust crossfeed design. Chapter III is the research procedure that was followed through this study. The research procedure describes the development of the robust crossfeed design from application to simple models of small variance to complex models of large variance. Chapter IV is an analysis of results comparing uncompensated, nominal, and robust off-axis response. This chapter presents time and frequency domain responses with an emphasis on statistical analysis. Chapter V contains conclusions and recommendations regarding the methods and results of the robust crossfeed design.

## CHAPTER II

### LITERATURE REVIEW

This chapter describes control theories and previous work that apply to this study. The foundation of this study, classical control theory, is used to address the issues of decoupling and robustness. Decoupling is accomplished through coupling numerator theory. Robustness is ensured through methods based on quantitative feedback theory. The crossfeed architecture is based on a control system proposed in ref. 3. A detailed description of how the previous work applies to this study follows.

#### *Coupling Numerator Theory*

The classical approach to crossfeed design uses coupling numerator theory, as explained in detail by McRuer et al., Jewell et al., and Hoh et al. (ref 4-6). The concept of "constrained variables" (see also ref. 7) is an important aspect of this approach. This concept allows the crossfeed design to take into account the approximate effects of the feedback loops not yet synthesized at this stage of the control system formulation. In the cited references, coupling numerator techniques were applied either to obtain crossfeeds for single design point models or to gain schedule as a function of key flight condition variables (e.g., airspeed, air density, gross weight, and vertical velocity as in ref. 5) but did not consider the problem of crossfeed design for highly uncertain systems. The current work combines coupling numerator theory with the QFT concept of uncertainty templates to yield an approach for robust crossfeed design.



### *Quantitative Feedback Theory*

A proposed concept for the RASCAL flight control system is based on the application of Quantitative Feedback Theory (QFT). QFT is a classically-based feedback control design method for robust compensation of uncertain plant transfer functions (ref. 8 - 10). The method is well suited to the rotorcraft flight control problem as described above because it directly addresses costs including actuator limiting, sensor noise amplification, and loss of stability robustness. The benefits of feedback are performance robustness, stability, and disturbance rejection.

In QFT, aircraft dynamics uncertainties are modeled in direct terms of gain and phase response variation ("uncertainty templates") associated with the family of design points to be included in the design as illustrated in fig. 2. As such, the QFT problem formulation is very well suited to the helicopter problem, where sophisticated simulations provide a large family of single point dynamic models as a function of physical parameters such as wind speed and direction, weight at hover, center of gravity location, moments-of-inertia, main rotor speed, and aircraft turn rate.

It is impractical to gain schedule the control system compensation as a function of the many parameters which affect aircraft dynamics; furthermore, many of these parameters are not measurable in-flight. Therefore, a large degree of uncertainty of aircraft dynamics will exist that must be included in the design. Dynamics variations are generally most significant for helicopter near-hovering flight, while control power is generally at a minimum level due to the lack of airspeed. These factors combine to make the hover condition flight control design a most challenging problem for the application of QFT techniques.

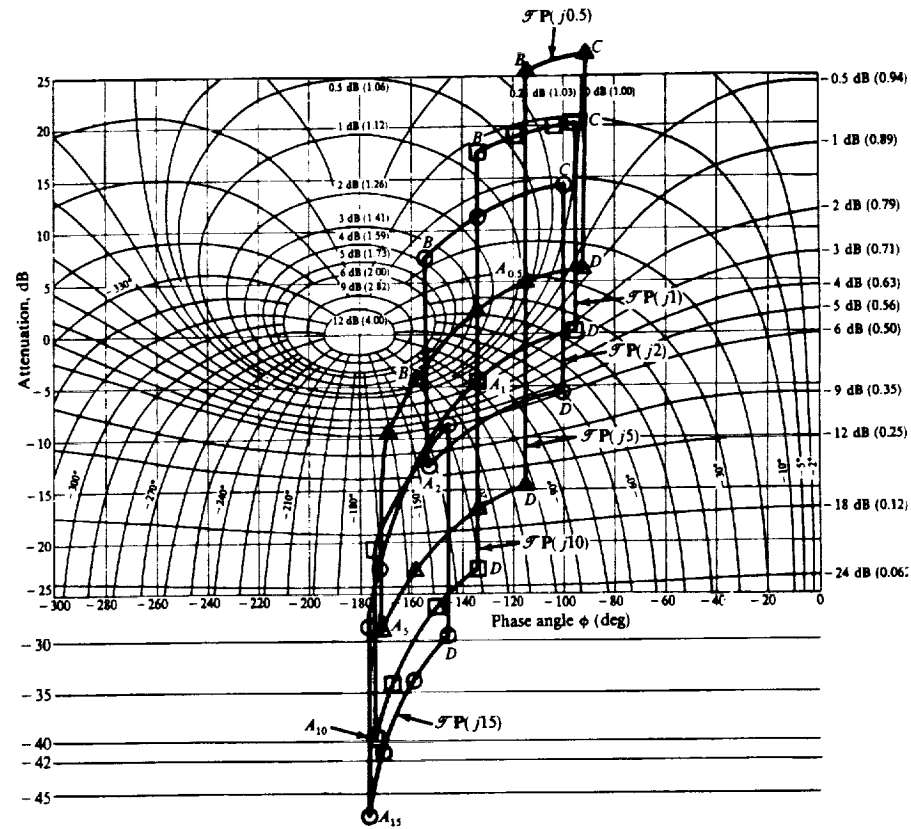


Figure 2 - QFT Design on the Nichols Plot

### Previous Related Work

The coupling numerator approach for crossfeed synthesis was first reviewed and demonstrated in ref. 3. This work addressed the pitch-roll coupling problem, which is a key source of coupling for most helicopter flight near hover. The new robust crossfeed design was explained and then applied to a design problem that considers five near-hover flight conditions. The performance of the robust crossfeed was shown to be superior to a conventional crossfeed based on a single point design model. The formulation and computer implementation of the new method allowed direct generalization to a relatively large number of flight conditions. Since, as discussed above, crossfeed pre-compensation is commonly used in helicopter flight control synthesis, the techniques presented in this paper are also applicable to design approaches other than QFT.

## CHAPTER III

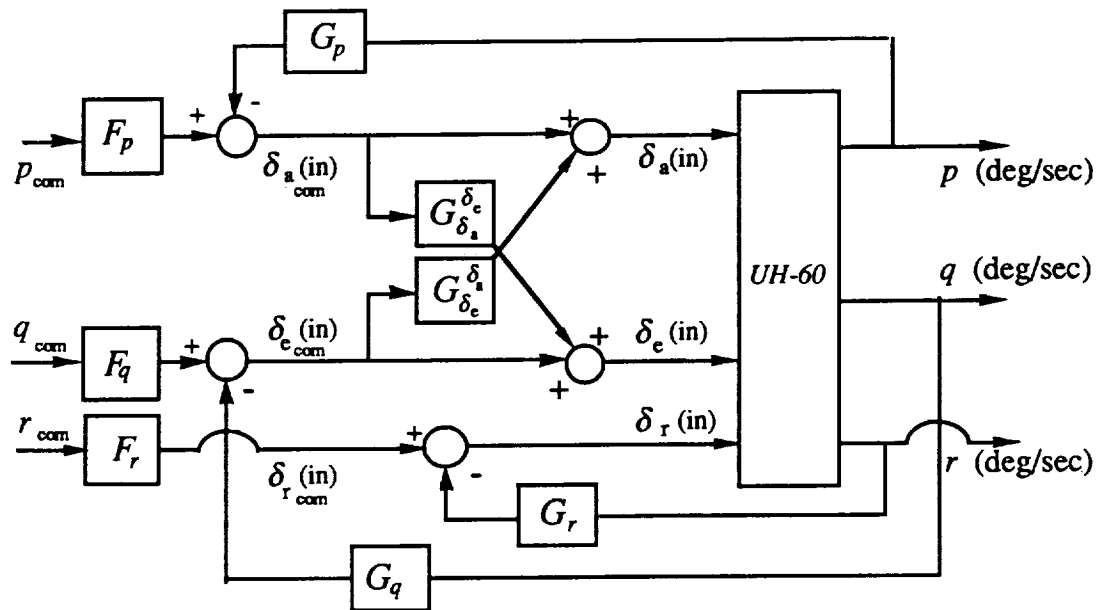
### RESEARCH PROCEDURE

The research procedure describes the development of the robust crossfeed design from application to simple models of small variance to complex models of large variance.

#### *Modeling of the Rotorcraft and Control System*

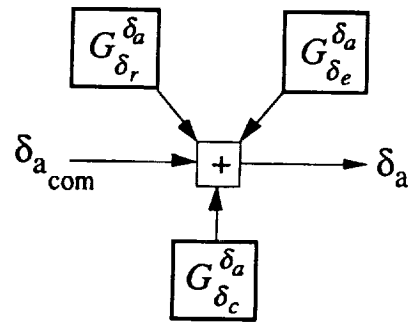
The current crossfeed design was extrapolated from ref. 3. This study will be revisited to assist in explaining basic concepts of the current crossfeed design.

Illustration of the pitch / roll decoupling problem ( 2 x 2 ). The overall control system structure for the 2 x 2 case shown in fig. 3. The vertical channel is not shown since it generally has a much lower bandwidth than the angular channels and thus is considered as an open-loop response. The 2 x 2 case considers only the key roll-to-pitch control crossfeed  $G_{\delta_r}^{\delta}$  (referred to herein as "pitch axis crossfeed") and pitch-to-roll control crossfeed  $G_{\delta_p}^{\delta}$  (referred to herein as "roll axis crossfeed"), but it does account for the presence of the yaw feedback compensation ( $G_r$ ). The crossfeed designs of this study are included in the bare-airframe dynamics to yield the "compensated open-loop response." With the mid- and high-frequency cross-coupling now effectively suppressed by the crossfeeds, QFT techniques can then applied to the compensated open-loop response to synthesize feedback and prefilter elements of the control system that satisfy the remaining design specifications. Derivation of the crossfeeds for the 2 x 2 case are shown in Appendix A.

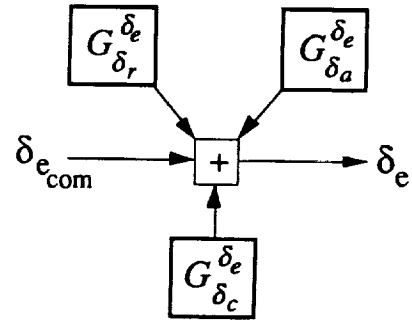


**Figure 3 - Control System Block Diagram**

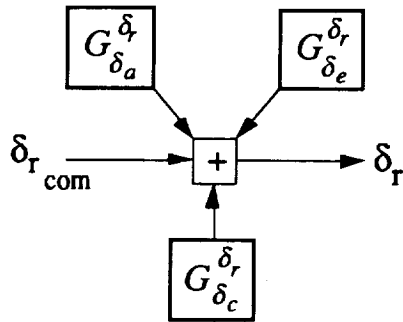
Explanation of the pitch / roll / yaw / heave decoupling problem ( 4 x 4 ). The 4x4 decoupling problem for 25 near-hover conditions was considered as a more realistic and complex problem than the 2x2 decoupling problem for 5 conditions that were previously investigated. Crossfeeds for the 4x4 decoupling problem are shown in fig. 4. The figure shows that it is possible to design 12 crossfeeds for the 4 x 4 system. However it is desired to identify which crossfeeds are necessary or possible to design. Analysis of bare airframe coupling assisted in this identification process.



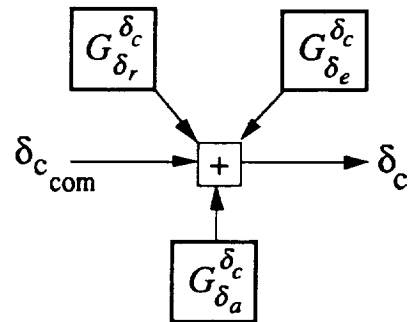
a) Crossfeeds to Lateral Cyclic



b) Crossfeeds to Longitudinal Cyclic



c) Crossfeeds to Tail Collective



d) Crossfeeds to Main Collective

**Figure 4 - Crossfeeds for the 4x4 System**

The rotorcraft mathematical model - UMGENHEL. High-order linear models of the UH-60 dynamics near hover are extracted from a comprehensive nonlinear simulation program (ref. 11). UMGENHEL is a methodically restructured and upgraded version of the original GENHEL helicopter blade-element simulation program (ref 12). The UMGENHEL linear models include dynamics of the fuselage, rotor, airmass, engine, and governor. Also represented is the control mixing, which provides limited decoupling through static crossfeeds. Since the control system actuators and digital component dynamics are symmetric in the pitch and roll axes, they do not affect the crossfeed calculations and therefore are not included in the model at this stage of the design.

Variation of configurations. Results presented in this paper are for a 6 degree-of-freedom (DOF), reduced-order (quasi-steady) UMGENHEL model. The simulation is capable of efficiently generating large families of linear models over a wide range of flight and configuration conditions. The current study includes the nominal hover operating point plus 24 off-nominal points. The 24 configurations include variations in trim airspeed (longitudinal and lateral), rotor RPM, aircraft weight and center of gravity, turning rate, climb speed, and descending speed. For this study, the configurations considered are shown in Appendix B. The configurations were put into groups of likelihood. Each group was given a weighting to signify the influence of each configuration in the group on crossfeed design and decoupling evaluation as shown in Table I. Group I was analyzed in ref. 3. Note that Groups I and II are given the same weighting.

**Table I. - Variation of Configurations**

<i>Group</i>	<i>Configurations</i>	<i>Weighting, <math>w_j</math></i>
<i>I Most Probable</i>	1-3, 7, 9	1.0
<i>II Less Probable</i>	6, 8, 14, 15	1.0
<i>III Least Probable</i>	4, 5, 10-13, 16-25	.3

The final crossfeed design will be based on the UMGENHEL model using the entire family of 25 configurations.

#### ***Uncompensated Response and Ideal Crossfeeds for the 4x4 Case***

Equations are shown here for calculating uncompensated on and off-axis rotorcraft responses which will be extensively used in later sections. The matrices of crossfeeds for all possible combinations of coupling is also shown.

Frequency range of interest for heave and rate responses. Frequency range of interest for rate commands ( $\delta_a$ ,  $\delta_e$ ,  $\delta_r$ ) was determined to be within 1 to 10 rad/sec. For

heave command ( $\delta_c$ ) the range of interest is .2 to 2. These ranges were determined experimentally from the autospectrum of pilot inputs during the ADOCS study (ref. 13). Note that 2-10 rad/sec was used in ref. 3. However 1-10 rad/sec. was used in this study.

Compensated response. The following compensated response equations are based on the coupling numerator theory that was proven for the 2 x 2 case. Details on the application of coupling numerators to the 4x4 case can be found in ref. 5. The equations are as follows:

**Table II - Lateral Cyclic,  $\delta_a$ , Input Responses**

Coupling	Off-Axis	On-Axis
pitch/roll (yaw constrained)	$\left. \frac{q}{\delta_a} \right _{\delta_c}^r = \frac{N_{\delta_a \delta_c}^{qr} + G_{\delta_c}^{\delta_a} N_{\delta_a \delta_c}^{qr} + G_{\delta_c}^{\delta_a} N_{\delta_a \delta_c}^{qr}}{N_{\delta_c}^r}$	$\left. \frac{p}{\delta_a} \right _{\delta_c}^r = \frac{N_{\delta_a \delta_c}^{pr}}{N_{\delta_c}^r}$
yaw/roll (pitch constrained)	$\left. \frac{r}{\delta_a} \right _{\delta_c}^q = \frac{N_{\delta_a \delta_c}^{rq} + G_{\delta_c}^{\delta_a} N_{\delta_a \delta_c}^{rq} + G_{\delta_c}^{\delta_a} N_{\delta_a \delta_c}^{rq}}{N_{\delta_c}^q}$	$\left. \frac{p}{\delta_a} \right _{\delta_c}^q = \frac{N_{\delta_a \delta_c}^{pq}}{N_{\delta_c}^q}$
heave/roll (pitch & yaw const.)	$\left. \frac{w}{\delta_a} \right _{\delta_c \delta_e}^{rq} = \frac{N_{\delta_a \delta_c \delta_e}^{wrq} + G_{\delta_c}^{\delta_a} N_{\delta_a \delta_c \delta_e}^{wrq}}{N_{\delta_c \delta_e}^{rq}}$	$\left. \frac{p}{\delta_a} \right _{\delta_c \delta_e}^{qr} = \frac{N_{\delta_a \delta_c \delta_e}^{pqr}}{N_{\delta_c \delta_e}^{qr}}$

**Table III - Longitudinal Cyclic,  $\delta_e$ , Input Responses**

Coupling	Off-Axis	On-Axis
roll/pitch (yaw constrained)	$\left. \frac{p}{\delta_e} \right _{\delta_c}^r = \frac{N_{\delta_e \delta_c}^{pr} + G_{\delta_c}^{\delta_e} N_{\delta_e \delta_c}^{pr} + G_{\delta_c}^{\delta_e} N_{\delta_e \delta_c}^{pr}}{N_{\delta_c}^r}$	$\left. \frac{q}{\delta_e} \right _{\delta_c}^r = \frac{N_{\delta_e \delta_c}^{qr}}{N_{\delta_c}^r}$
yaw/pitch (roll constrained)	$\left. \frac{r}{\delta_e} \right _{\delta_c}^p = \frac{N_{\delta_e \delta_c}^{rp} + G_{\delta_c}^{\delta_e} N_{\delta_e \delta_c}^{rp} + G_{\delta_c}^{\delta_e} N_{\delta_e \delta_c}^{rp}}{N_{\delta_c}^p}$	$\left. \frac{q}{\delta_e} \right _{\delta_c}^p = \frac{N_{\delta_e \delta_c}^{qp}}{N_{\delta_c}^p}$
heave/pitch (roll & yaw const.)	$\left. \frac{w}{\delta_e} \right _{\delta_c \delta_a}^{pr} = \frac{N_{\delta_e \delta_c \delta_a}^{wpr} + G_{\delta_c}^{\delta_e} N_{\delta_e \delta_c \delta_a}^{wpr}}{N_{\delta_c \delta_a}^{pr}}$	$\left. \frac{q}{\delta_e} \right _{\delta_c \delta_a}^{pr} = \frac{N_{\delta_e \delta_c \delta_a}^{qpr}}{N_{\delta_c \delta_a}^{pr}}$

Table IV - Tail rotor collective,  $\delta_r$ , Input Responses

Coupling	Off-Axis	On-Axis
pitch/yaw (roll constrained)	$\left. \frac{q}{\delta_r} \right _{\delta_s}^p = \frac{N_{\delta_s \delta_s}^{qp} + G_{\delta_s}^{\delta_s} N_{\delta_s \delta_s}^{qp} + G_{\delta_s}^{\delta_s} N_{\delta_s \delta_s}^{qp}}{N_{\delta_s}^p}$	$\left. \frac{r}{\delta_r} \right _{\delta_s}^p = \frac{N_{\delta_s \delta_s}^{rp}}{N_{\delta_s}^p}$
roll/yaw (pitch constrained)	$\left. \frac{p}{\delta_r} \right _{\delta_s}^q = \frac{N_{\delta_s \delta_s}^{pq} + G_{\delta_s}^{\delta_s} N_{\delta_s \delta_s}^{pq} + G_{\delta_s}^{\delta_s} N_{\delta_s \delta_s}^{pq}}{N_{\delta_s}^q}$	$\left. \frac{r}{\delta_r} \right _{\delta_s}^q = \frac{N_{\delta_s \delta_s}^{rq}}{N_{\delta_s}^q}$
heave/yaw (roll & pitch const.)	$\left. \frac{w}{\delta_r} \right _{\delta_s \delta_s}^{pq} = \frac{N_{\delta_s \delta_s}^{wpq} + G_{\delta_s}^{\delta_s} N_{\delta_s \delta_s}^{wpq}}{N_{\delta_s \delta_s}^{qp}}$	$\left. \frac{r}{\delta_r} \right _{\delta_s \delta_s}^{pq} = \frac{N_{\delta_s \delta_s}^{rpq}}{N_{\delta_s \delta_s}^{qp}}$

Table V - Main Rotor Collective,  $\delta_c$ , Input Responses

Coupling	Off-Axis	On-Axis
pitch/heave (roll & yaw const.)	$\left. \frac{q}{\delta_c} \right _{\delta_s \delta_s}^{pr} = \frac{N_{\delta_s \delta_s}^{qpr} + G_{\delta_s}^{\delta_s} N_{\delta_s \delta_s}^{qpr}}{N_{\delta_s \delta_s}^{pr}}$	$\left. \frac{w}{\delta_c} \right _{\delta_s \delta_s}^{pr} = \frac{N_{\delta_s \delta_s}^{wpr}}{N_{\delta_s \delta_s}^{pr}}$
roll/heave (pitch & yaw const.)	$\left. \frac{p}{\delta_c} \right _{\delta_s \delta_s}^{qr} = \frac{N_{\delta_s \delta_s}^{pqr} + G_{\delta_s}^{\delta_s} N_{\delta_s \delta_s}^{pqr}}{N_{\delta_s \delta_s}^{qr}}$	$\left. \frac{w}{\delta_c} \right _{\delta_s \delta_s}^{rq} = \frac{N_{\delta_s \delta_s}^{wrg}}{N_{\delta_s \delta_s}^{rq}}$
yaw/heave (roll & pitch const.)	$\left. \frac{r}{\delta_c} \right _{\delta_s \delta_s}^{pq} = \frac{N_{\delta_s \delta_s}^{rpq} + G_{\delta_s}^{\delta_s} N_{\delta_s \delta_s}^{rpq}}{N_{\delta_s \delta_s}^{qp}}$	$\left. \frac{w}{\delta_c} \right _{\delta_s \delta_s}^{pq} = \frac{N_{\delta_s \delta_s}^{wpq}}{N_{\delta_s \delta_s}^{qp}}$

Recall 25 configurations were linearized. These linearizations result in a unique characteristic equation for each type of constraint. These characteristic equations and their respective coupling numerators may be found using software for control systems analysis such as LCAP (ref. 14).



Ideal crossfeed calculation for the 4x4 system. The ideal crossfeeds for the 4x4 system can be expressed in matrices having the form :

$$\mathbf{P}\bar{\mathbf{m}} = \bar{\mathbf{y}}$$

Where  $\mathbf{P}$  is a square matrix of coupling numerators,  $\bar{\mathbf{m}}$  is a vector of crossfeeds, and  $\bar{\mathbf{y}}$  is a vector of coupling numerators. The ideal crossfeed matrices are shown below:

Lateral cyclic,  $\delta_a$ , crossfeeds:

$$\begin{bmatrix} N_{\delta_a\delta_a}^{\theta r} & 0 & N_{\delta_a\delta_a}^{\theta r} \\ N_{\delta_a\delta_a}^{r\theta} & N_{\delta_a\delta_a}^{r\theta} & 0 \\ N_{\delta_a\delta_a}^{w\theta r} & 0 & 0 \end{bmatrix} \begin{bmatrix} G_{\delta_a}^{\delta_a} \\ G_{\delta_a}^{\delta_a} \\ G_{\delta_a}^{\delta_a} \end{bmatrix} = \begin{bmatrix} -N_{\delta_a\delta_a}^{\theta r} \\ -N_{\delta_a\delta_a}^{r\theta} \\ -N_{\delta_a\delta_a}^{w\theta r} \end{bmatrix}$$

Longitudinal cyclic,  $\delta_e$ , crossfeeds:

$$\begin{bmatrix} N_{\delta_e\delta_e}^{\theta r} & N_{\delta_e\delta_e}^{\theta r} & 0 \\ 0 & N_{\delta_e\delta_e}^{r\theta} & N_{\delta_e\delta_e}^{r\theta} \\ 0 & N_{\delta_e\delta_e}^{w\theta r} & 0 \end{bmatrix} \begin{bmatrix} G_{\delta_e}^{\delta_e} \\ G_{\delta_e}^{\delta_e} \\ G_{\delta_e}^{\delta_e} \end{bmatrix} = \begin{bmatrix} -N_{\delta_e\delta_e}^{\theta r} \\ -N_{\delta_e\delta_e}^{r\theta} \\ -N_{\delta_e\delta_e}^{w\theta r} \end{bmatrix}$$

Tail rotor collective,  $\delta_r$ , crossfeeds:

$$\begin{bmatrix} N_{\delta_r\delta_r}^{\theta\theta} & 0 & N_{\delta_r\delta_r}^{\theta\theta} \\ 0 & N_{\delta_r\delta_r}^{\theta\theta} & N_{\delta_r\delta_r}^{\theta\theta} \\ 0 & 0 & N_{\delta_r\delta_r}^{w\theta\theta} \end{bmatrix} \begin{bmatrix} G_{\delta_r}^{\delta_r} \\ G_{\delta_r}^{\delta_r} \\ G_{\delta_r}^{\delta_r} \end{bmatrix} = \begin{bmatrix} -N_{\delta_r\delta_r}^{\theta\theta} \\ -N_{\delta_r\delta_r}^{\theta\theta} \\ -N_{\delta_r\delta_r}^{w\theta\theta} \end{bmatrix}$$

Main rotor collective,  $\delta_c$ , crossfeeds:

$$\begin{bmatrix} N_{\delta_c\delta_c}^{\theta\theta r} & 0 & 0 \\ 0 & N_{\delta_c\delta_c}^{\theta\theta r} & 0 \\ 0 & 0 & N_{\delta_c\delta_c}^{r\theta\theta} \end{bmatrix} \begin{bmatrix} G_{\delta_c}^{\delta_c} \\ G_{\delta_c}^{\delta_c} \\ G_{\delta_c}^{\delta_c} \end{bmatrix} = \begin{bmatrix} -N_{\delta_c\delta_c}^{\theta\theta r} \\ -N_{\delta_c\delta_c}^{\theta\theta r} \\ -N_{\delta_c\delta_c}^{r\theta\theta} \end{bmatrix}$$

Crossfeed vectors can be determined through matrix inversion:

$$\bar{\mathbf{m}} = \mathbf{P}^{-1}\bar{\mathbf{y}}$$

Details of the ideal crossfeed derivation can be found in ref. 5.

### *Low-Order Approximation of the Ideal Crossfeeds*

Highlights of ref. 3 are presented here to explain the development of low order fits to ideal crossfeeds.

Characteristics of the ideal crossfeed. Using the coupling numerator relationships and, the ideal crossfeeds for the nominal (#1) configuration are:

$$G_{\delta_s}^{\delta_s}(\#1) = -\frac{N_{\delta_s \delta_s}^{q r}}{N_{\delta_s \delta_s}^{q r}} = \frac{0.571(0.966)(.503E-03)(-.695E-02)(.26)(23.6)}{16.6(-.143E-01,.519)(-.171E-03)(-.26E-01)(.263)(4.06)}$$

and

$$G_{\delta_s}^{\delta_s}(\#1) = -\frac{N_{\delta_s \delta_s}^{p r}}{N_{\delta_s \delta_s}^{p r}} = \frac{2.98(.0541,.833)(.0362)(.264)(-8.16)(0)}{65.6(-.253,.489)(.0222)(.264)(.949)(0)}$$

which were obtained using the LCAP controls analysis program . Note that these "ideal" crossfeeds have unstable poles, and so are not practical. Practical, stable dynamic crossfeeds are obtained by approximating the ideal crossfeeds with low-order equivalent transfer functions over the frequency range of interest (2-10 rad/sec). The low-order crossfeed fit results obtained from NAVFIT (ref. 15) are summarized for the nominal configuration in table VI. These crossfeeds are simple first and second order functions with stable (i.e. physically practical) dynamic modes.

**Table VI. Approximations to the Ideal Crossfeeds for the Nominal Configuration**

Type of Fit	$G_{\delta_s}^{\delta_s}(\#1) = -\frac{N_{\delta_s \delta_s}^{q r}}{N_{\delta_s \delta_s}^{q r}}$	$G_{\delta_s}^{\delta_s}(\#1) = -\frac{N_{\delta_s \delta_s}^{p r}}{N_{\delta_s \delta_s}^{p r}}$
<i>Low Order</i>	$\frac{-.817}{(4.54)}$	$\frac{49.5}{[.351, 11.8](.2)}$

Low-order crossfeed fit to a nominal ideal crossfeed. In QFT loop-shaping terminology, the performance characteristics of a crossfeed apply not only to a single design configuration but to a “specified set” of configurations. This single crossfeed, appropriately selected for a set of configurations, is called in this study the “target” compensation, and the low-order (LO) approximation to this “target” is called the “achieved” compensation.

Figure 5 is a Bode plot for configuration #1 showing the accuracy of the low-order dynamic approximation to the ideal crossfeed  $G_{\delta_a}^{\delta_c}(\#1)$ . The simple low-order dynamic crossfeed  $G_{\delta_a}^{\delta_c}(\#1_{LO})$  matches the ideal result very well over part of the frequency range of concern (1 to 10 rad/sec). It would be expected that decoupling performance for this crossfeed would be better for the 2 - 10 rad/sec. range than the 1 - 2 rad/sec. range.

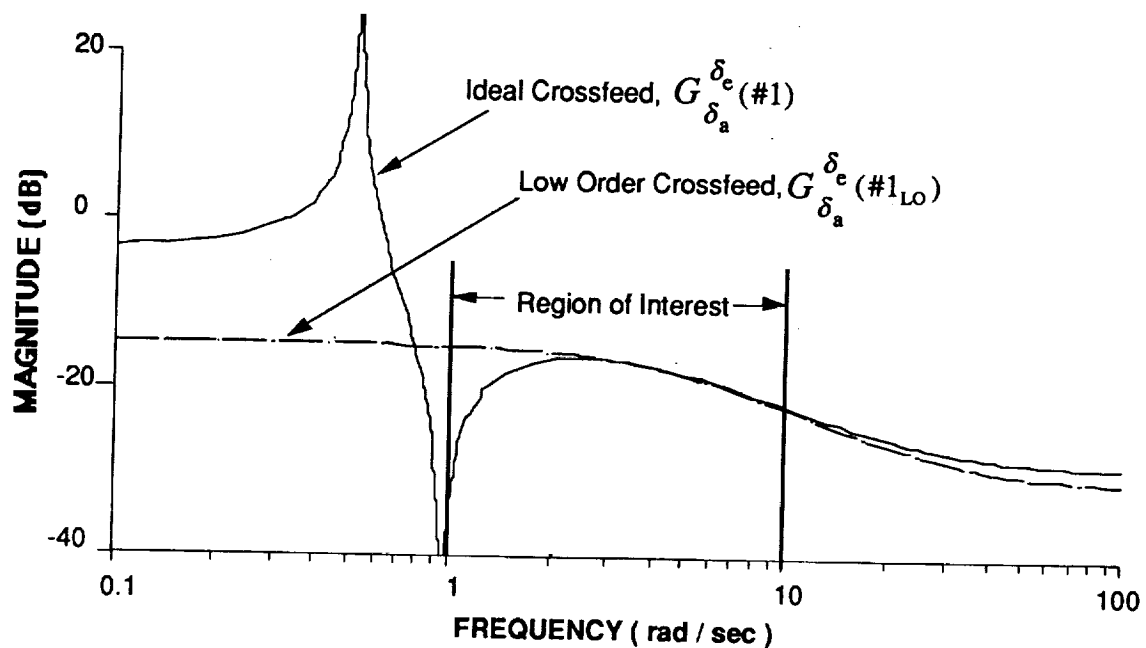


Figure 5 - Low Order Fit to Ideal Crossfeed

### ***Decoupling Performance Metric***

Evaluation of robust decoupling for a set of configurations. If a crossfeed is doing its job properly, then the off-axis frequency responses of the family of configurations will be substantially attenuated over the frequencies of concern " $\omega_i$ ". The array of off-axis response magnitudes for each of the " $j$ " configurations are obtained at these " $i$ " frequencies and denoted by  $M_{off,i,j}$  in dB. The magnitude of the off-axis response is conveniently normalized relative to a baseline *on-axis* response to yield a measure of relative decoupling. The choice of which configuration to use for this baseline is arbitrary since we are mostly concerned with comparative improvements in decoupling for various strategies. In this paper the nominal configuration (#1) is established as the baseline configuration, and is denoted by  $M_{on,i,1}$  in dB at each frequency " $\omega_i$ ". The average decoupling of one configuration over  $m$  frequencies is as follows:

$$\Delta M_j = \frac{\sum_{i=1}^m (M_{on,i,1} - M_{off,i,j})}{m} \text{ (dB)}$$

The decoupling at  $m$  frequencies "averaged" over  $n$  configurations is expressed (for each axis) by the metric:

$$J_{avg} = \frac{\sum_{j=1}^n w_j \Delta M_j}{\sum_{j=1}^n w_j} \text{ (dB)}$$

This metric is defined as average decoupling. Configuration weighting is also utilized to give Groups I and II more value in decoupling.

Uncompensated off-axis transfer functions were compared to on-axis magnitudes to determine if a crossfeed was necessary for that response. Using the performance metric based on average magnitude for all conditions, any response having a metric greater than 20 dB did not need a crossfeed.

Consideration of coupling variance. Another objective is to reduce coupling while minimizing the variance in off-axis response. Variance was measured with the following cost function based on the standard deviation of coupling response:

$$J_{\sigma} = \sqrt{\frac{\sum_{j=1}^n w_j^2 \left( \frac{\Delta M_j}{w_j} - J_{avg} \right)^2}{\sum_{j=1}^n w_j^2}} \quad (\text{dB})$$

The cost of variance was subtracted from average decoupling to determine a metric that takes into account robustness and decoupling effectiveness:

$$\underline{J_{total} = J_{avg} - J_{\sigma}} \quad (\text{dB})$$

This metric is defined as the robust decoupling metric. It is desired to make the robust decoupling metric as large as possible when designing robust crossfeeds.

### ***Graphical Basis for Robust Crossfeed Design***

The strategy developed in ref. 3 was patterned after QFT graphical techniques that use the Nichols chart for presentation of "target" compensation, "achieved" compensation, and configuration variations in gain and phase ("templates"). For example, fig. 6 compares the Nichols chart representation of the low-order crossfeed  $G_{\delta_e}^{\delta_i}(\#1_{LO})$  with that of the "ideal" crossfeed  $G_{\delta_e}^{\delta_i}(\#1)$  for the nominal hover configuration. This figure is simply a replot of the lower-order dynamic crossfeed results from fig 5 (including the phase data). The "ideal" crossfeed based on the nominal configuration is shown with the symbol "+" for five frequency points over the 2-10 rad/sec frequency range of interest. The five frequency points are logarithmically-spaced,  $\{\omega_i\} = \{2.0, 3.0, 4.47, 6.68, 10.0 \text{ rad/sec}\}$ . The (small)

mismatches of the ideal and lower-order crossfeeds are clearly visible for this frequency range. Gain and phase values for "ideal" crossfeeds based on the other remaining four configurations may also be depicted on the Nichols chart at each of the frequency points. Fig. 6 shows the result for a frequency of 2 rad/sec. This collection of "ideal" gain and phase values at a specified frequency is called a "crossfeed template" and may be connected with lines for useful visual effect.

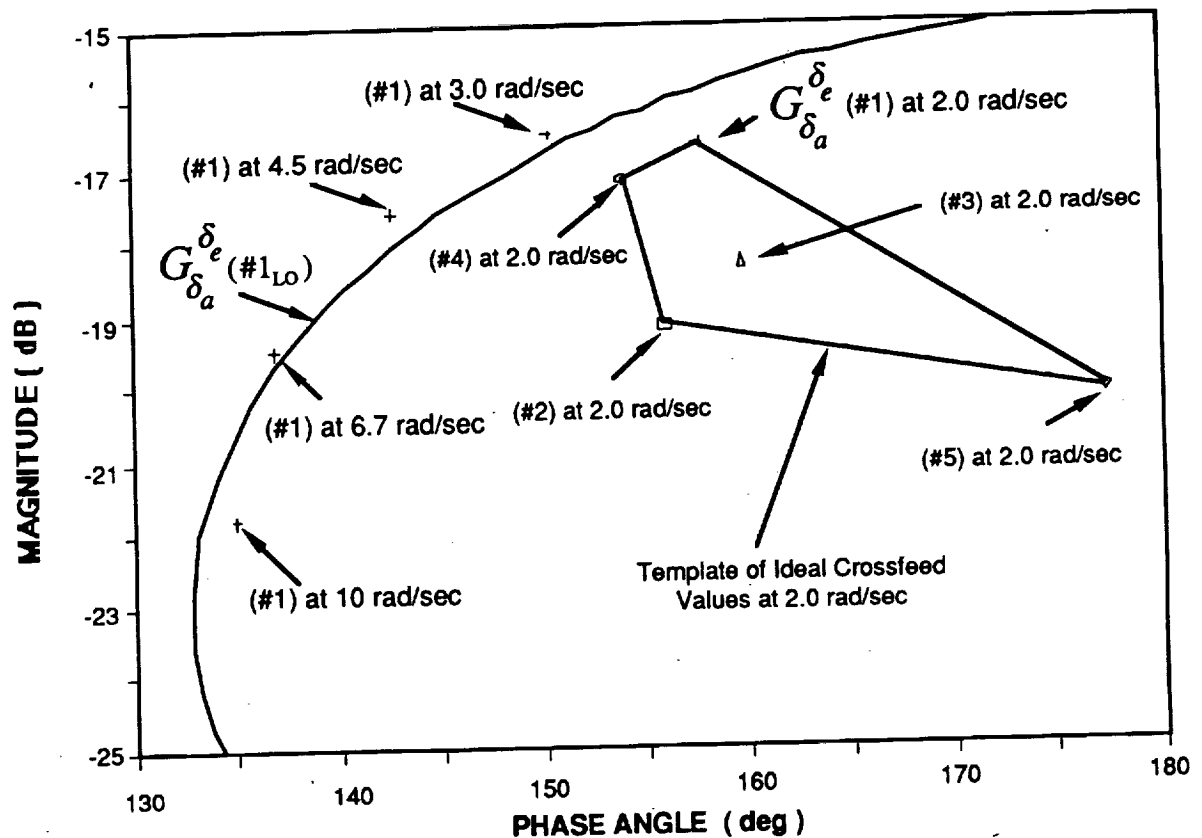


Figure 6 - Nichols Chart Representation of Low-Order Approximation

The  $G_{\delta_e}^{\delta_a}$  crossfeed template for each of the five frequency points is shown in fig. 7. Each template depicts the variability of the "ideal" crossfeeds over the family of plant configurations. In the earlier crossfeed design, the "target" gain and phase values used in the low-order fit process were those associated with the ideal solution for the nominal configuration (#1) denoted with the symbol "+" on each template. This is obviously the best

solution for decoupling the nominal plant dynamics. However, an inspection of fig. 7 shows that a design that closely tracks the ideal crossfeed solution for configuration #1,  $G_{\delta_e}^{\delta}(\#1)$ , will be quite far from the crossfeed solution for configuration 5, and may in fact worsen the coupling behavior for this configuration. Therefore, the question now is whether there is a better strategy for selecting a "target" point in each template that will result in improved overall decoupling performance.

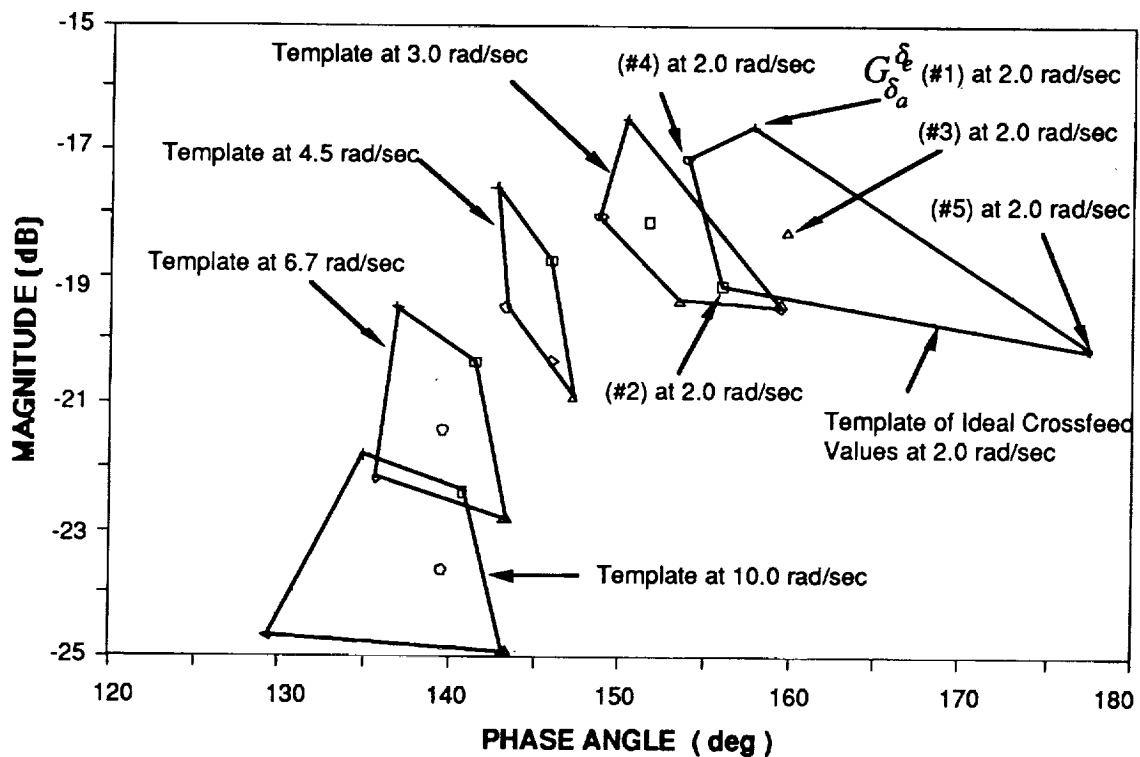


Figure 7 - Frequency Templates of Ideal Crossfeeds  $G_{\delta_e}^{\delta}$

The following crossfeed design strategy makes use of the ideal crossfeed templates.

### *The Mean Square Weighting Strategy*

The heuristic strategy recommended in the previous study is called "mean-square weighting" (MSW) decoupling. The first step in this strategy is to find a "target" crossfeed point (gain/phase location) on each template that is a weighted-average which favors a cluster of points within a given template. Then, the lower-order fitting technique is used to design a crossfeed to best match these target points. Weights in the fitting program are chosen so that the crossfeed design matches more closely the target points associated with the templates having a smaller size -- where the proper choice of desired target value is well defined and should be ensured. When the template is large in size, the weights are reduced since the exact location of the crossfeed is not as well defined.

Target crossfeeds. In the previous example, the "target" crossfeed values used in the fitting process were chosen based on the "ideal" crossfeed solutions for configuration #1 (nominal). Many heuristic strategies for selecting appropriate target values were also considered in this study. Referring to fig. 8, one obvious method would be to select target values based on the average of each crossfeed template.



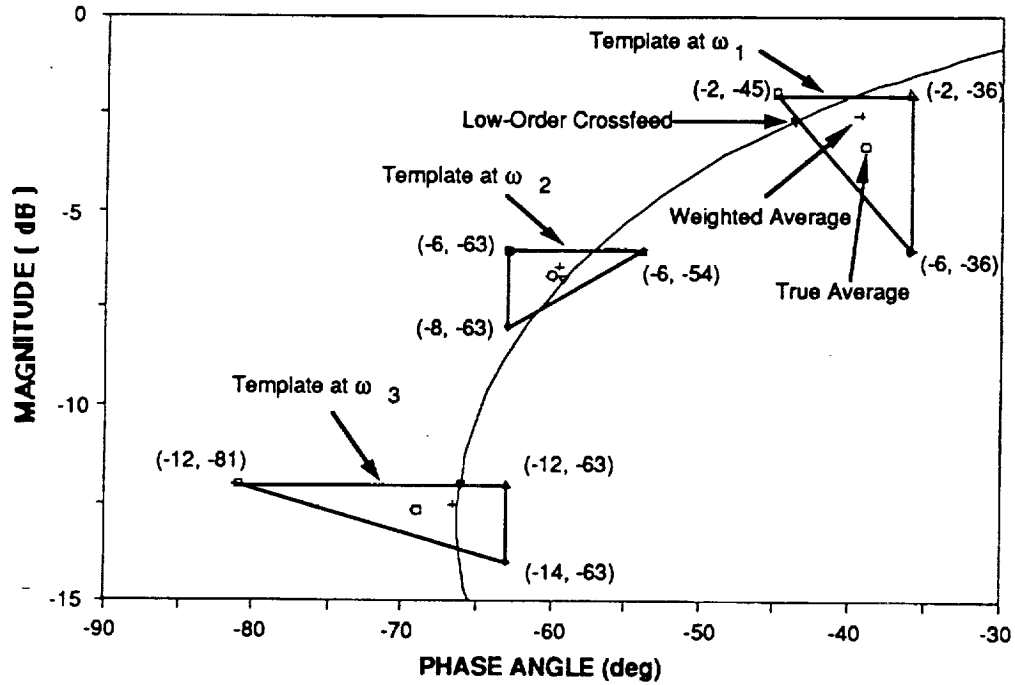


Figure 8 - MSW Strategy with Synthesized Templates

To implement the MSW strategy, first determine the average gain and phase point (dB and degrees) for each template  $|G(avg)|$  and  $\angle G(avg)$ . The difference between the average gain and phase of a template and the "ideal crossfeed" gain and phase for each configuration (j) in the template gives the gain and phase deviations for the template "i". Now looping over all the template frequencies gives arrays as a function of i and j:

$$\Delta M_{i,j} = \{|G(\#j)| - |G(avg)|\}_i \quad \text{dB}$$

$$\Delta \phi_{i,j} = \{\angle G(\#j) - \angle G(avg)\}_i \quad \text{deg}$$

The mean square weight for the point (i,j) is defined as:

$$w_{msw,i,j} = \min[1, \{ \frac{1}{\Delta M_{i,j}^2 + 0.01745(\Delta \phi_{i,j})^2} \}]$$

where the weighting of 7.6 deg of phase to 1dB is adopted as recommended in practice (ref 17).

The MSW "target" crossfeed point for the template "i" is defined as:

$$M_{MSW,i} = \frac{\sum_{Conf j} w_j w_{msw,i,j} |G(\#j)|_i}{\sum_{Conf j} w_j w_{msw,i,j}} \quad \text{and} \quad \phi_{MSW,i} = \frac{\sum_{Conf j} w_j w_{msw,i,j} \angle G(\#j)_i}{\sum_{Conf j} w_j w_{msw,i,j}}$$

**Frequency weighting.** The lower-order "fit" to the above "target" crossfeed points is found by using the following weights in the NAVFIT program at frequency "i":

$$w_{NAVFIT,i} = \min[1, \{ \frac{1}{\sigma_{mag,i}^2 + 0.01745(\sigma_{phase,i})^2} \}]$$

where

$$\sigma_{mag,i}^2 = \frac{1}{m} \sum_{Conf j=1,n} \{|G(\#j)| - |G(avg)|\}_i^2 \quad \text{and} \quad \sigma_{phase,i}^2 = \frac{1}{m} \sum_{Conf j=1,n} \{\angle G(\#j) - \angle G(avg)\}_i^2$$

A sample calculation of weights is provided in table VII for the artificial data in fig. 8.

Template 2 has the highest relative weighting because the template points are more highly clustered than the other templates.

**Table VII - Sample Target Crossfeed Values**

Template 'i'	$ G(avg) _i$	$\angle G(avg)_i$	$M_{MSW,i}$	$\phi_{MSW,i}$	$w_{NAVFIT,i}$
1	-3.33	-39.0	-2.52	-39.5	.51
2	-6.67	-60.0	-6.42	-59.6	1.00
3	-12.67	-69.0	-12.50	-66.6	.92

### ***Template Analysis***

Ideal crossfeed templates for each off-axis response were plotted with the ideal crossfeed points for the 25 flight conditions. Target crossfeed points were generated using the MSW strategy. Recall that for the 5 flight condition case, templates enclosed all of the ideal crossfeeds for one frequency. However, the 25 configuration case requires that influential points be identified for each frequency in order to generate graphical templates useful for robust low-order crossfeed design.

Influential points. It was necessary to identify influential points in each template. This was done by evaluating the sensitivity of the MSW target crossfeed for a certain template by moving an ideal crossfeed point  $\pm 1$  dB or  $\pm 10$  deg. and then recalculating the MSW target crossfeed. If the MSW target crossfeed moves  $\pm 0.05$  dB or  $\pm 0.5$  deg. the ideal crossfeed point is considered influential. Influential points are included in the template shape for each frequency.

Robust regression and outlier detection. In ref. 17 outlier detection and robust regression are compared. Identification of influential points is a method of outlier detection. Ideal crossfeed points that are not outliers contribute significantly to the target crossfeed solution. The MSW strategy is a method of robust regression. The MSW strategy generates target crossfeeds despite the presence of outliers. Ref. 17 emphasizes that robust regression and outlier detection are different ways to achieve a similar result. Therefore target crossfeed estimates were calculated using influential points and the MSW strategy.

Condition for non-existence of a practical low-order crossfeed. Determination of "most influential" points assists in the judgment of whether a crossfeed is effective for certain frequencies. A rule of thumb that was established is that if a template of "most

influential" ideal crossfeeds overlaps the target points of other frequencies, a low-order dynamic crossfeed would not decouple effectively at the frequency of the template. If the target points are close in magnitude and phase, and each template is small, a static crossfeed may decouple effectively over all the frequencies of interest. These observations were confirmed from the following template analysis.

Template analysis results for the 4x4 case. Fig. 9 - 11 show the template analysis for necessary crossfeeds. Frequency templates, target crossfeeds, and the low order crossfeed fit, if appropriate, is shown on a Nichols Chart of each crossfeed analysis. The discussion of each figure lists configurations that were influential on the target crossfeed generation. The average of the more influential configurations in each frequency template is presented along with the target crossfeed to show that they are close in magnitude and phase. Table VIII identifies features of the crossfeed templates.

**Table VIII - Features of the Crossfeed Templates**








Symbol	Feature
	$\omega_1$
	$\omega_2$
	$\omega_3$
	$\omega_4$
	$\omega_5$
	Target Crossfeed Point
	Static Crossfeed Fit

Fig. 9 is the plot of templates containing influential ideal crossfeed points for  $G_{\delta_c}^{\delta_c}$ . There was judged to be no practical low-order crossfeed for this set of templates because the template shapes are large in relation to the small dispersion of the target crossfeeds,

indicating excessive variation in the crossfeed data. Also the target crossfeeds are centered near -90 degrees of phase which rejects the possibility of using a static crossfeed.

Configuration influence data for this crossfeed is shown in table IX.

**Table IX - Configuration Influence for  $G_{\delta_e}^{\delta_s}$**

$\omega_1$	Configurations	Target Mag.	Target Phase	Appx. Mag.	Appx. Phase
.20	2,3,6,7,8,9,11,16	-19.4	-51.5	-16.2	-50.5
.36	8	-21.4	-74.2	-21.8	-74.2
.63	2,3,4,5,6,8,9,15,17, 18,19,23,24	-20.5	-69.5	-19.8	-66.4
1.13	2,3,5,8,15,17,18,19	-22.4	-73.4	-22.8	-72.5
2.00	2,3,5,18,19	-26.0	-70.9	-25.5	-77.7

Approximate magnitude and phase are determined by the average of influential points for each frequency. It may be inferred from the data that large variance in crossfeed data is indicated by large differences between target and approximate data. For example the difference at  $\omega_1$  is 3.2 dB. Differences for the other frequencies are at least .4 dB.

Fig. 10 shows the templates of influential ideal crossfeeds for  $G_{\delta_e}^{\delta_s}$ . A low-order crossfeed was possible for this set of templates. The low-order crossfeed is shown on the figure as the solid line passing through the templates close to the target crossfeeds.

Configuration influence data for this crossfeed is shown in table X.

**Table X - Configuration Influence for  $G_{\delta}^{\delta}$** 

$\omega_1$	Configurations	Target Mag.	Target Phase	Appx. Mag.	Appx. Phase
1.00	2,6,7,9,24	-16.9	-69.1	-16.7	-66.6
1.78	1,2,6,7,9,14,15,24	-17.0	-72.8	-16.5	-72.6
3.16	1,2,6,7,8,9,10,11, 14,15,16,20,24,25	-19.7	-78.8	-19.4	-72.5
5.62	1,2,6,7,9,10,11,15, 16,20,24	-23.0	-82.2	-23.3	-86.5
10.00	1,2,6,7,8,9,10,11, 12,14,15,16,17,18, 20,24	-25.0	-81.9	-26.0	-87.0

The differences in magnitude between target and approximate values are at most .5 dB except for  $\omega_5$ . However it is obvious from the figure that  $\omega_5$  has the largest variance because it has the largest size template on the Nichols plot.

Fig. 11 shows the templates of influential ideal crossfeeds for  $G_{\delta}^{\delta}$ . It was possible to fit a static crossfeed to these templates because the target crossfeeds vary little in magnitude and are within 20 deg. of -180 deg phase. Configuration influence data for this crossfeed is shown in table XI.

**Table XI - Configuration Influence for  $G_{\delta}^{\delta}$** 

$\omega_1$	Configurations	Target Mag.	Target Phase	Appx. Mag.	Appx. Phase
.20	1,2,3,4,5,7,8,9,15, 21	-13.8	163.8	-14.1	157.3
.36	1,3,8,9,13,15,21,	-14.1	162.9	-14.5	160.9
.63	1,2,3,8,9,12,15,21	-15.6	164.3	-15.9	164.4
1.13	2,3,8,9,15,19	-16.7	168.7	-16.6	169.4
2.00	2,3,6,8,9,19	-17.4	173.0	-17.8	174.1

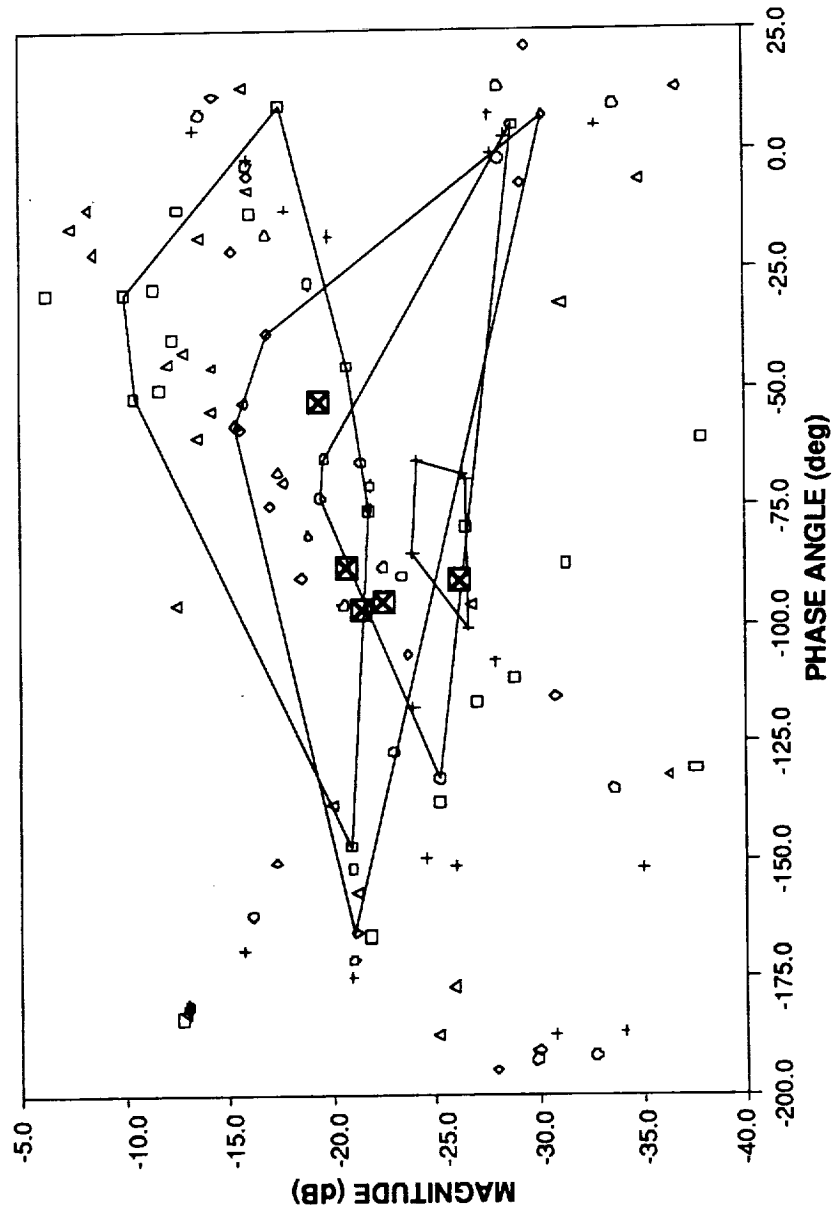


Figure 9 - Templates of Influential Ideal Crossfeed Points for  $G_{\delta_c}^{\delta_a}$

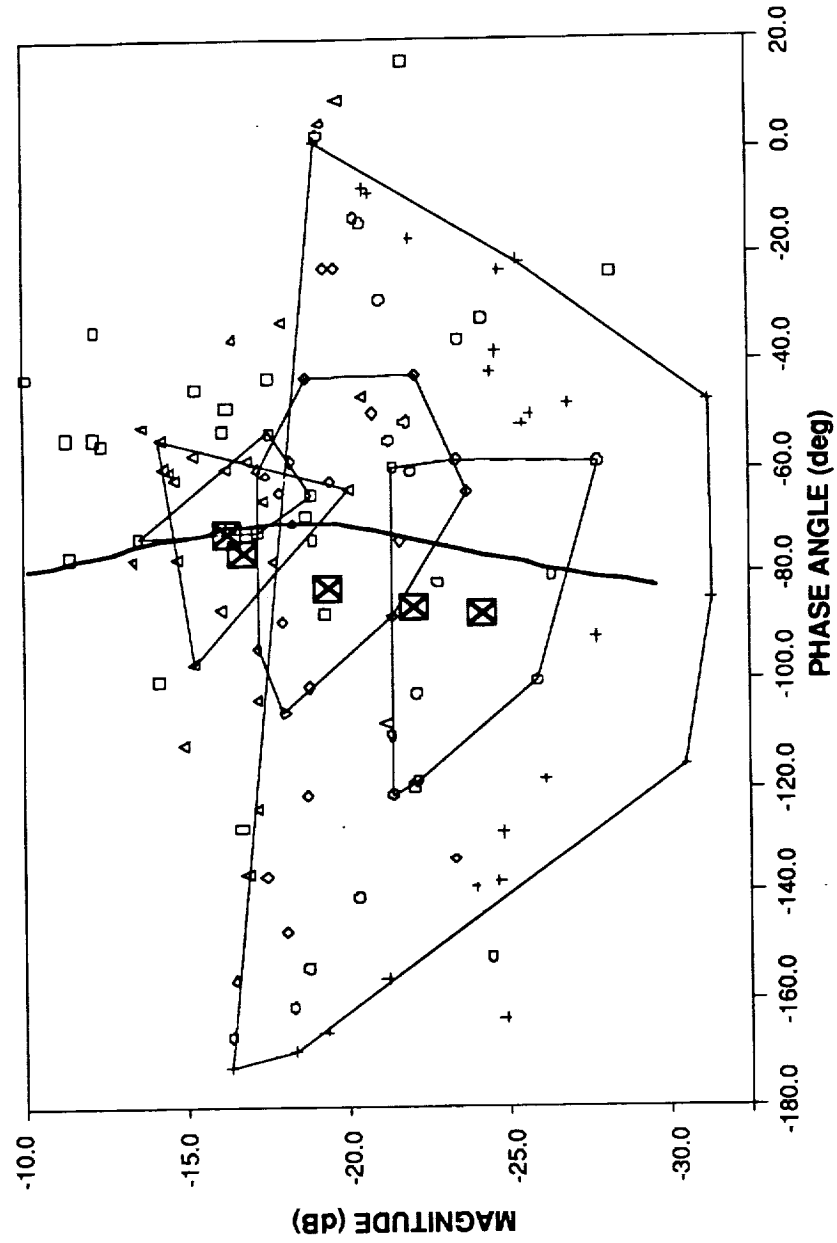


Figure 10 - Templates of Influential Ideal Crossfeed Points for  $G_{\delta_e}^a$



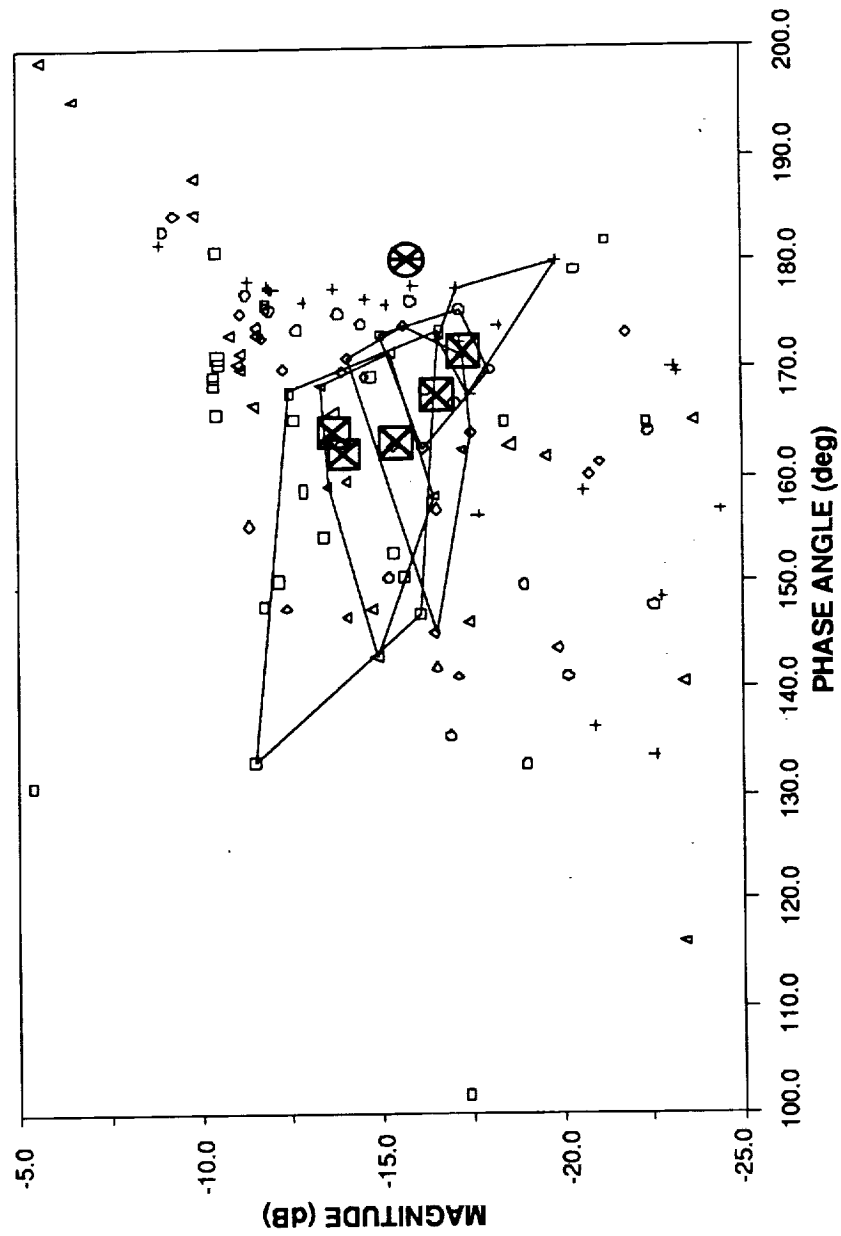


Figure 11 - Templates of Influential Ideal Crossfeed Points for  $G_{\delta_c}^{\delta_r}$

## CHAPTER IV

### ANALYSIS OF RESULTS

The purpose of this section is show how the effectiveness of any crossfeed strategy may be evaluated through the analysis of magnitudes for compensated responses. This analysis starts with a statistical approach to evaluate robustness and concludes with frequency and time domain techniques associated with traditional control systems evaluation. Throughout this analysis,  $p / \delta_e$  and  $r / \delta_c$  responses will be examined to compare methods of evaluating the effectiveness of the MSW strategy.

#### *Summary of Crossfeed Compensation*

Table XII is a result of applying the  $J_{avg}$  average decoupling metric to all the bare airframe degrees-of-freedom.

**Table XII. Average Metrics**

$J_{avg, uncomp.}$	$p$	$q$	$r$	$w$
$\delta_a$	on-axis	26.5 (u)	22.1 (u)	33.3 (u)
$\delta_e$	13.3 (d)	on-axis	24.6 (u)	26.6 (u)
$\delta_r$	3.2 (s)	23.6 (u)	on-axis	31.0 (u)
$\delta_c$	19.3 (np)	17.5 (d)	8.0 (s)	on-axis

The letters by each metric indicate the crossfeed strategy for each response:

(u) - uncompensated, no crossfeed necessary

(s) - static crossfeed

(d) - dynamic crossfeed

(np) - crossfeed not practical due to excessive variance in mag and phase

Crossfeed design was considered for off-axis responses with average decoupling under 20 dB and possible use of practical low-order crossfeeds. Table XIII shows the MSW crossfeeds generated for the off-axis responses requiring static or dynamic crossfeeds.

**Table XIII - Summary of MSW Crossfeeds**

<i>Off-Axis Response</i>	<i>Crossfeed</i>	<i>MSW fit</i>	<i>Nominal fit</i>
$\frac{p}{\delta_e}$	$G_{\delta_e}^{\delta_e}$	$\frac{.446(1.49)}{(0)(3.47)}$	$\frac{49.5}{[.351, 11.8](.2)}$
$\frac{q}{\delta_c}$	$G_{\delta_c}^{\delta_c}$	$\frac{.043(2.53)}{(.30)}$	-.817
$\frac{p}{\delta_r}$	$G_{\delta_r}^{\delta_r}$	.476	.467
$\frac{r}{\delta_c}$	$G_{\delta_c}^{\delta_r}$	-.135	-.202

### **Performance Improvement Summary**

Use of a nominal crossfeed vs. the MSW crossfeed is shown on the following table. The robust decoupling metric is defined as:  $J_{total} = J_{avg} - J_{\sigma}$ . This metric represents a "worst case" representation of coupling for a certain crossfeed. Table XIV shows all metrics for the compensated off-axis responses.

**Table XIV - Compensated Off-Axis Metrics**

<i>Response</i>	<i>Metric</i>	<i>Uncomp.</i>	<i>Nominal</i>	<i>MSW</i>
$\frac{p}{\delta_e}$	$J_{avg}$	13.2	15.4	16.4
	$J_{\sigma}$	2.7	4.3	4.3
	$J_{total}$	10.5	11.1	12.1
$\frac{q}{\delta_c}$	$J_{avg}$	15.8	22.6	18.7
	$J_{\sigma}$	5.3	15.7	7.4
	$J_{total}$	10.8	7.0	11.3

Table XIV - Compensated Off-Axis Metrics ( cont.)

$\frac{p}{\delta_r}$	$J_{avg}$	3.2	20.2	19.7
	$J_{\sigma}$	1.4	5.4	5.1
	$J_{total}$	1.8	14.7	14.5
$\frac{r}{\delta_c}$	$J_{avg}$	8.0	13.9	15.1
	$J_{\sigma}$	4.5	3.1	3.8
	$J_{total}$	3.5	10.8	11.3

Each of the MSW compensated responses show improvement from nominal and uncompensated values of robust decoupling. The significance of this improvement is shown in various graphical formats.

#### Scatter Plots

The difference in standard deviation between uncompensated, nominal, and MSW response can best be visualized on scatter plots, which are shown on fig. 12 and 13. The scatter plots show how  $\Delta M_j$  varies with configuration. Each plot shows  $J_{avg}$  as a solid line. The dashed lines above and below the average are  $J_{avg} \pm J_{\sigma}$ . The lower standard deviation line corresponds to  $J_{total}$ . The filled circles signify Group I and II configurations for which decoupling is highly weighted. The open squares signify Group III configurations which decoupling is given lower weighting.

Fig. 12 shows the scatter plots for  $p / \delta_c$  compensation. It was observed that configurations 3 and 14 benefit the most from nominal compensation to MSW compensation. However this improvement was at the expense of configurations 1 and 15.

Fig. 13 shows the scatter plots for  $r / \delta_c$  compensation. It was observed that decoupling was decreased on Group III configurations 20, 22, 24, and 25 as a result of improving the decoupling of several Group I and II configurations.

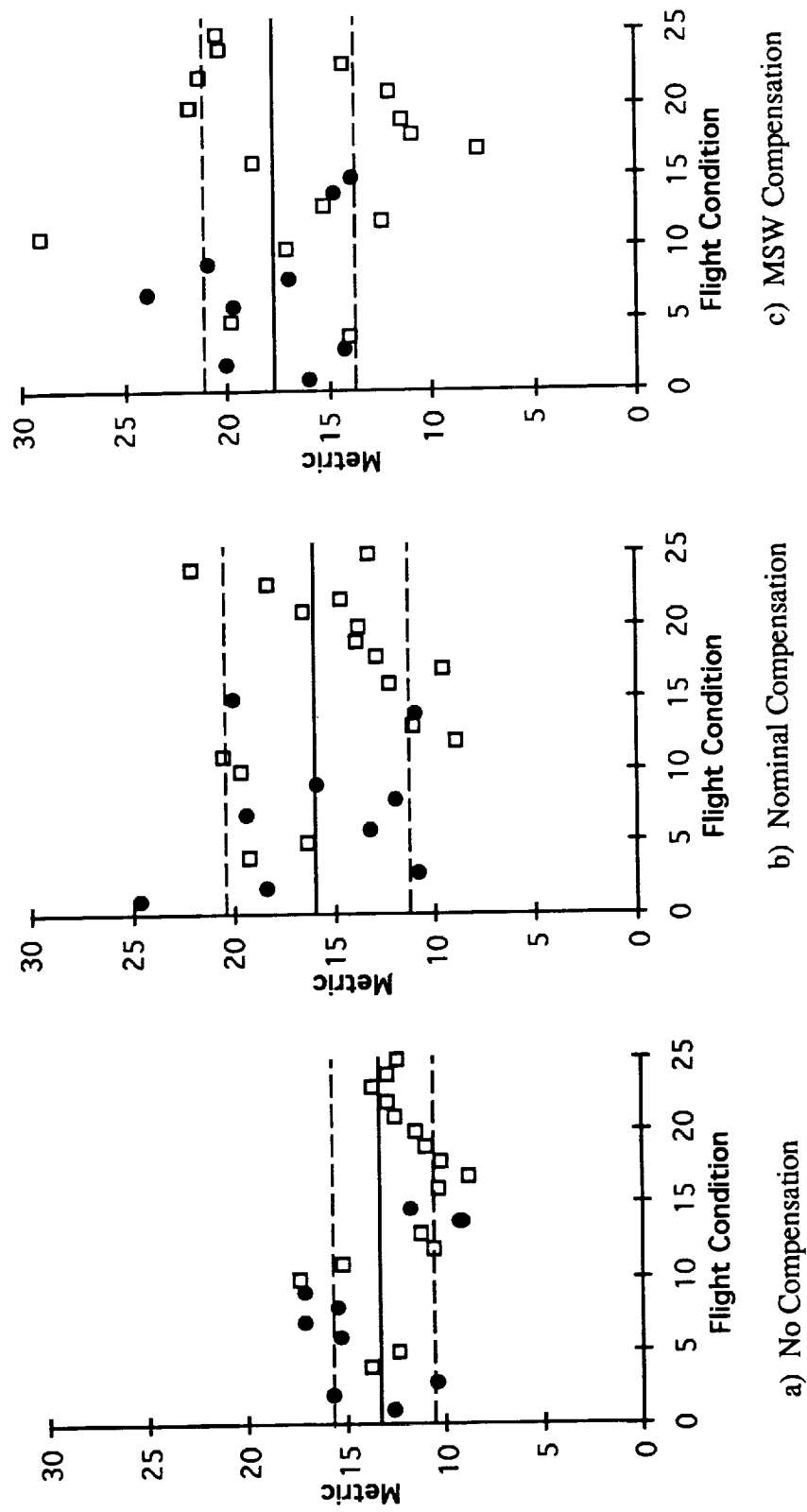
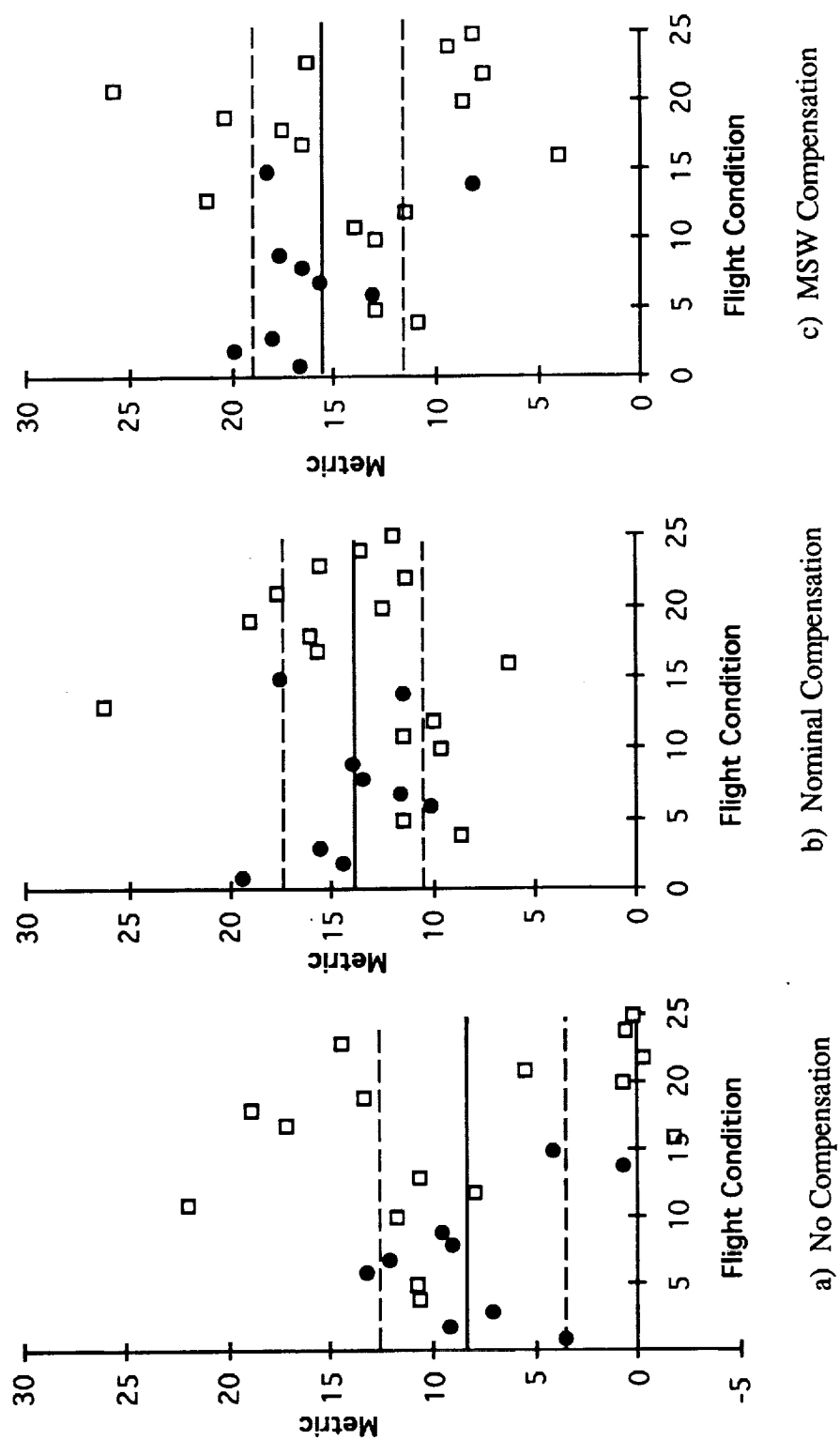


Figure 12 - Comparison of Decoupling Averages for  $p / \delta_e$

Figure 20 - Comparison of Decoupling Averages for  $r / \delta_c$

Scatter plots allow the crossfeed designer to see which configurations benefit the most from a certain crossfeed strategy. If a certain configuration does not reach a desired level of decoupling due to a crossfeed strategy, it may be weighted higher on the next design iteration.

### ***Bode Plots***

The performance metric shows improvement in decoupling in magnitude over the frequency range of interest. To see how decoupling improves over certain frequencies, magnitude response is presented on Bode plots shown in fig. 14 - 17. The average magnitude of all the configurations across the frequencies is shown as a solid line. To illustrate to variance of coupling with flight condition  $\pm\sigma$  magnitudes are plotted for each frequency.  $+\sigma$  magnitude is shown as a dashed line.  $-\sigma$  magnitude is shown as a dash-dot line. Table XV shows the symbols that are used to signify what compensation was used on the Bode plot.

**Table XV - Bode Plot Features**

<i>Symbol</i>	<i>Compensation</i>
□	uncompensated
●	nominal
△	MSW

Fig. 14 and 15 show the  $p / \delta_e$  compensation comparison on Bode plots. Fig. 14 shows that the improvement in decoupling occurs in the middle of the frequency range of interest (2-6 rad/sec). Fig. 15 shows that the MSW crossfeed minimizes coupling variance, especially near 2 rad/sec. This demonstration of decoupling effectiveness within the frequency of interest shows that the crossfeed strategy will work for the expected bandwidth of pilot input rather than at the edge of it.

Fig. 16 and 17 show the  $r / \delta_c$  compensation comparison on Bode plots. Fig. 16 shows that the most improvement in decoupling occurs at the high end of the frequency range of interest (.6 - 2.0 rad/sec). Fig. 17 shows that the MSW crossfeed exhibits its robustness at the high end of the frequency range also. Notice that the variance of the MSW response is greater at .2 rad/sec. At higher frequencies, the MSW decoupling equals the nominal decoupling in variance and has a greater average.

The Bode plots of the average and variance of decoupling show the range of frequencies at which the robust crossfeed was effective.

### ***Time Response Plots***

Time response plots were generated for flight conditions representative of the average and variance of decoupling. This was accomplished by determining the unit step response of configurations representative of  $J_{avg} \pm J_{\sigma}$  and  $J_{avg}$  which were shown in the scatter plots. Each response was passed through a low-pass filter to better visualize crossover frequency characteristics and normalized by the nominal on-axis response. Roll/pitch coupling was filtered with 10/(10). Yaw/heave coupling was filtered with 2/(2). This procedure results in coupling percentage vs. time. Absolute values were taken of coupling percentage to easily visualize magnitude of coupling. The line type vs.  $J_{avg} \pm J_{\sigma}$  and  $J_{avg}$  that was established for the scatter plots applies to the time responses also.



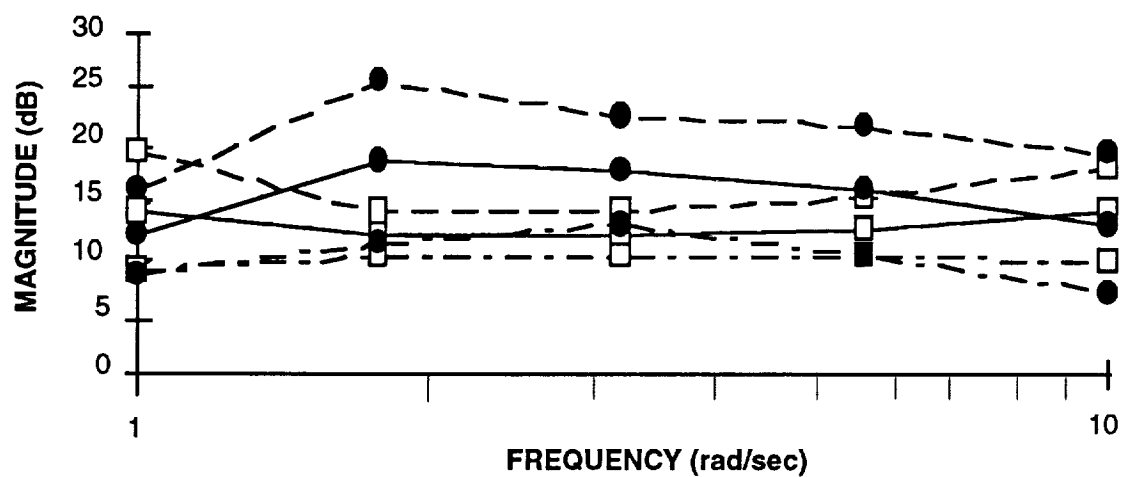


Figure 14 - Nominal vs. Uncompensated Metric Bode Plot:  $p / \delta e$

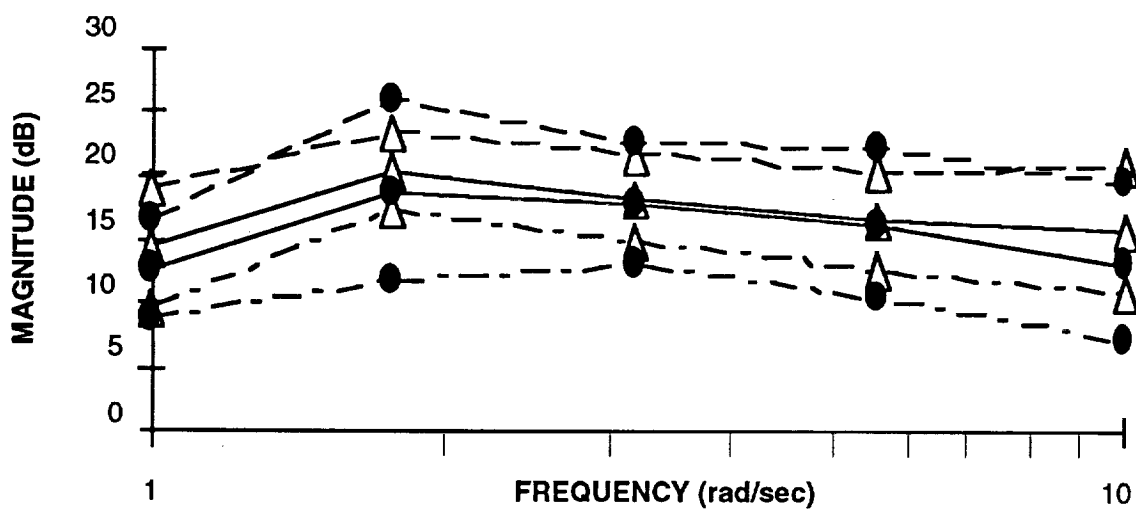


Figure 15 - Nominal vs. MSW Metric Bode Plot:  $p / \delta e$

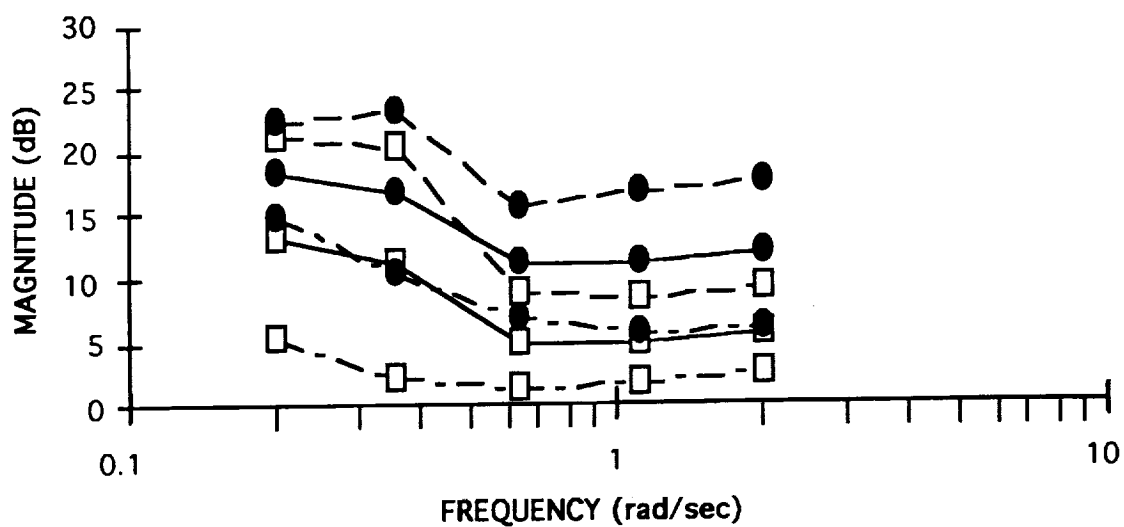


Figure 16 - Nominal vs. Uncompensated Metric Bode Plot:  $r / \delta_c$

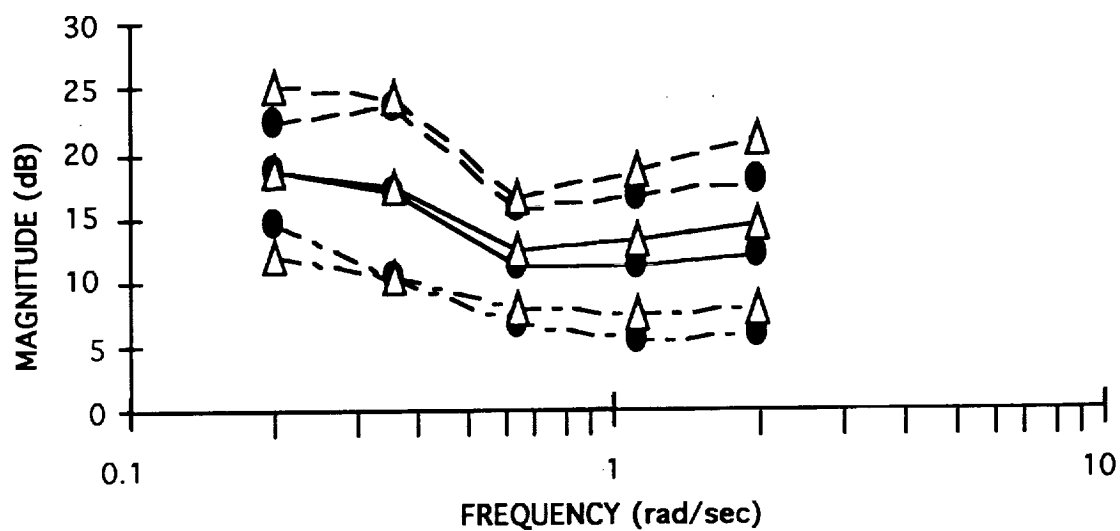


Figure 17 - Nominal vs. MSW Metric Bode Plot:  $r / \delta_c$

Fig. 18 and 19 show the uncompensated responses for roll/pitch and yaw/heave respectively. Different time scales were chosen to present each coupling because they were generated from different frequency ranges of interest. Fig 20 and 21 show the nominal responses. Fig 22 and 23 show the MSW responses. It was observed that coupling specifications are usually stated in terms of a peak coupling within a certain time from initial input (ref. 2). The time response results for roll/pitch coupling was reported to be the peak coupling within .5 sec for either of the  $J_{avg} \pm J_{\sigma}$  or  $J_{avg}$  configurations. For yaw/heave coupling, the result was reported to be the peak coupling within 1 sec. This would reflect the lower frequency range of interest for yaw/heave coupling. Tables XVI and XVII show tabular results for robust decoupling in the time domain.

**Table XVI - Representative Time Response for Roll/Pitch Coupling**

<i>Comp.</i>	<i>Configuration</i>			% peak at $t < .5 \text{ sec.}$
	$J_{avg}$	$J_{avg} - J_{\sigma}$	$J_{avg} + J_{\sigma}$	
uncomp.	23	12	2	.28
nominal	9	13	11	.21
MSW	10	15	22	.13

**Table XVII - Representative Time Response for Yaw/Heave Coupling**

<i>Comp.</i>	<i>Configuration</i>			% peak at $t < 1 \text{ sec.}$
	$J_{avg}$	$J_{avg} - J_{\sigma}$	$J_{avg} + J_{\sigma}$	
uncomp.	8	1	7	.59
nominal	9	22	15	.26
MSW	7	12	3	.23

The configurations listed can be traced back to the scatter plots. The peak values for the time scales for each type of coupling indicate improvement in robust decoupling for the representative set of configurations.

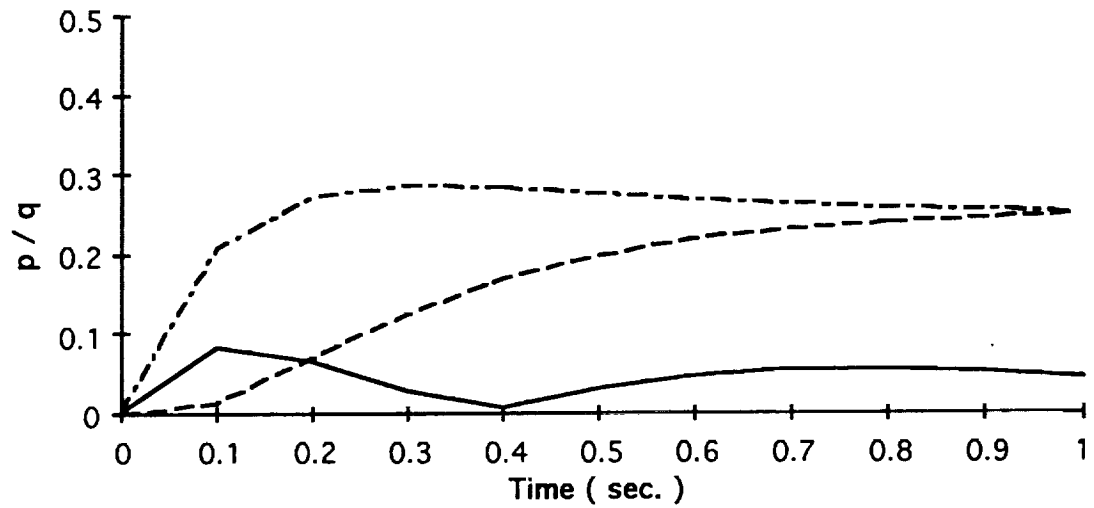


Figure 18 - Uncompensated Time Response: Roll / Pitch

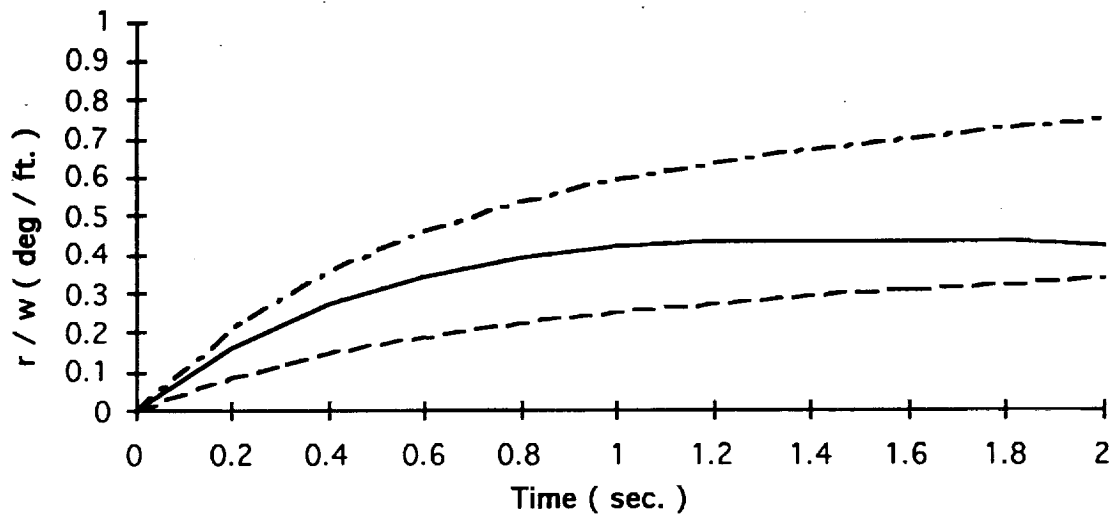


Figure 19 - Uncompensated Time Response: Yaw / Heave

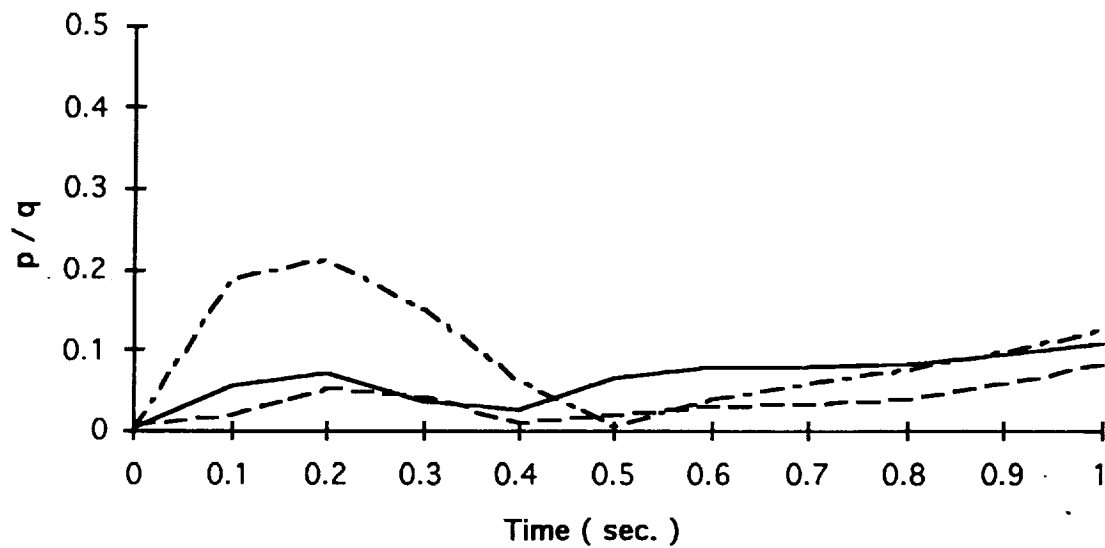


Figure 20 - Nominal Time Response: Roll / Pitch

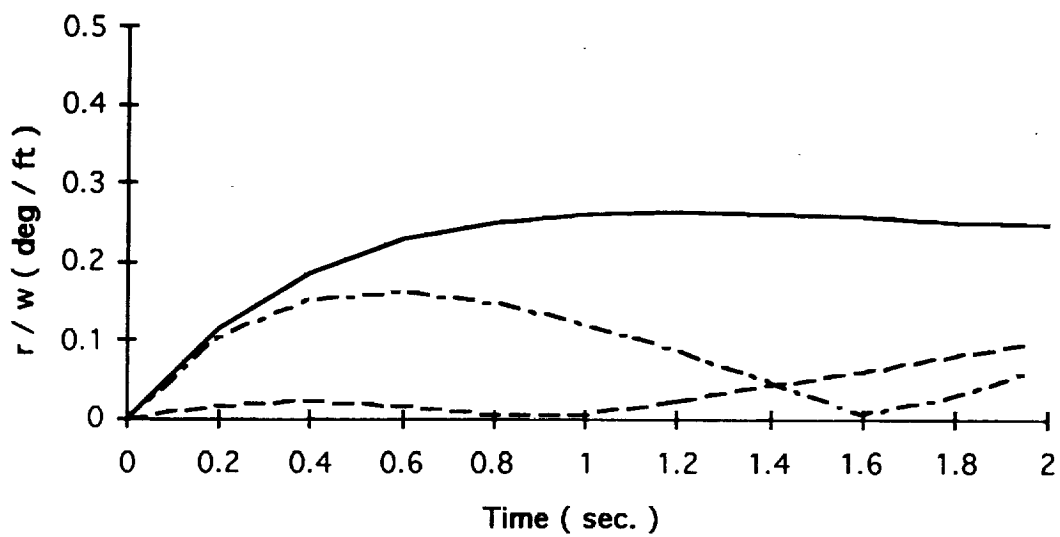


Figure 21 - Nominal Time Response: Yaw / Heave

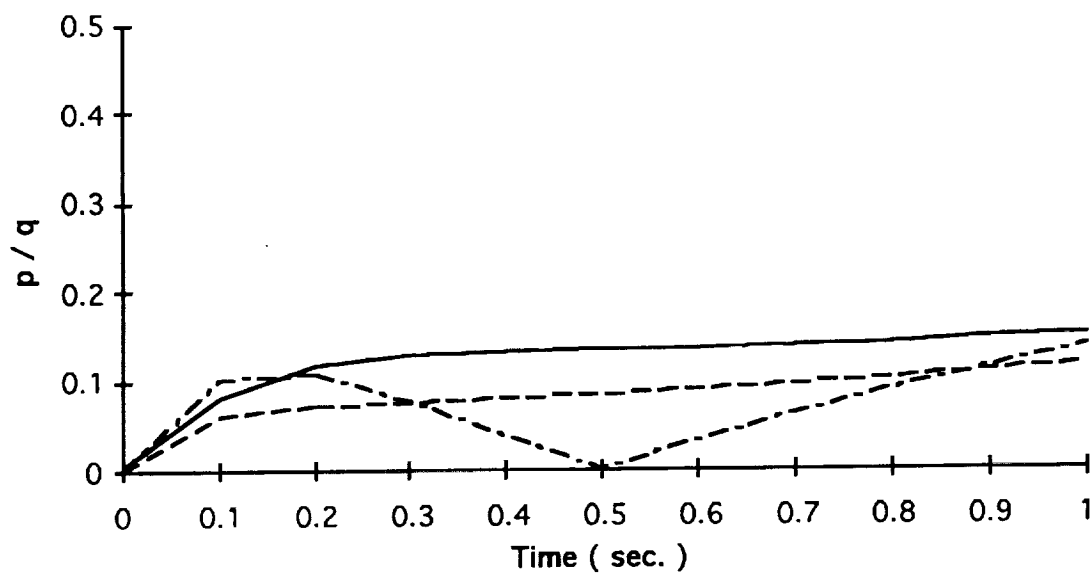


Figure 22 - MSW Time Response: Roll / Pitch

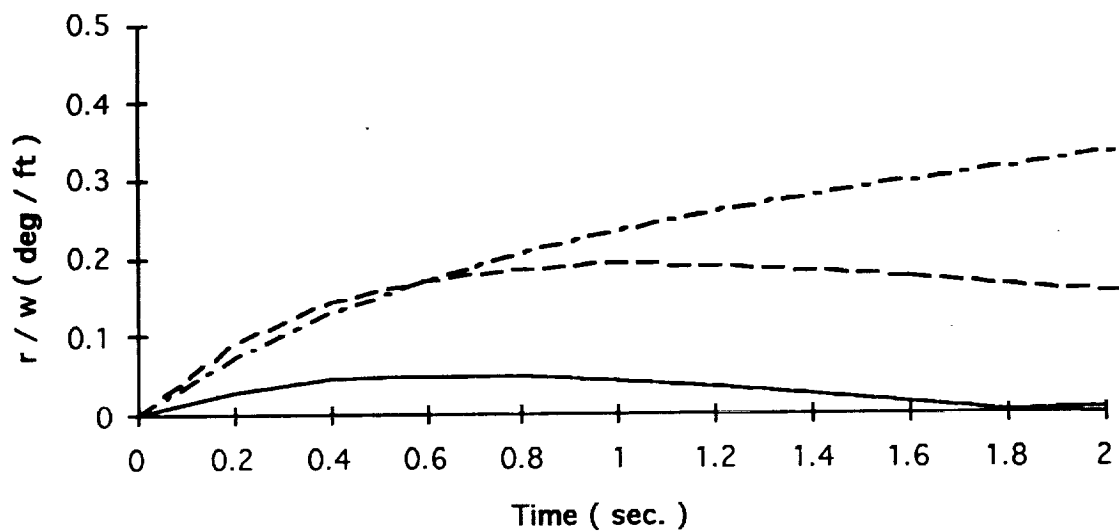


Figure 23 - MSW Time Response: Yaw / Heave

## **CHAPTER V.**

### **CONCLUSIONS**

A graphical method was developed to determine if a low-order crossfeed is feasible for attenuation of off-axis response for a set of flight conditions:

1. The MSW strategy is one method of crossfeed design that may result in a robust crossfeed for a set of flight conditions.
2. Analysis of influential points on each template determines if the MSW strategy will result in an effective crossfeed.
3. Four crossfeeds were designed, one crossfeeds was not achievable, seven crossfeeds were not necessary for the 4x4 case.
  - a. One crossfeed not achievable due to high template variance.
  - b. Two crossfeeds are static as a result of the rotorcraft model not having engine dynamics.

A performance metric was developed to evaluate robust decoupling through analysis of average and standard deviation of off-axis magnitude response:

1. Off-axis response for nominal and MSW crossfeeds were compared to see how configuration variance affects the robust decoupling metric.
2. The performance metric can be graphically represented by scatter plots of average off-axis magnitude response for each flight condition.

The crossfeed design and performance metric make use of graphical techniques which lend significant physical insight into the design procedure. The crossfeed design method can be easily automated and allows detection of configurations that are influential on the design. The low-order crossfeeds reduced coupling significantly for the set of configurations that were analyzed.

A recommendation for further work includes analysis of robust low-order crossfeed design for higher-order models. Also reduction of feedback gains by using robust low-order crossfeeds should be compared with feedback designs that do not use crossfeeds.



## REFERENCES

- 1) Aiken, E. W., Hindson, W. S., Lebacqz, J. V., Denery, D. G., Eshow, M. M.,  
"Rotorcraft In-Flight Simulation Research at NASA Ames: A Review of the 80s  
and Plans for the 90's." *International Symposium on In-Flight Simulation for the  
1990's*. Braunschweig, Federal Republic of Germany. July 1991.
- 2) U. S. Army. *Aeronautical Design Standard - Handling Qualities Requirements for  
Military Rotorcraft*. ADS-33C. August 1989.
- 3) Catapang, D., Tischler, M., Biezad, D. "Robust Crossfeed Design for Hovering  
Rotorcraft." *Quantitative Feedback Theory Symposium Proceedings*. USAF  
Document WL-TR-92-3063. Wright-Patterson AFB. August 1992.
- 4) McRuer, D. T. , Ashkenas, I. L., and H. R. Pass. *Analysis of Multi-loop Vehicular  
Control Systems*. ASR-TDR-62-1014. Wright-Patterson Air Force Base, Ohio.  
March 1964.
- 5) Jewell, W. F., Clement, W. F. *Crossfeed Compensation Techniques for Decoupling  
Rotorcraft Responses to Control Inputs*. TR-1229-1. Systems Technology, Inc.  
September 1985.

- 6) Hoh, R. H., Myers, T. T., Ashkenas, I. L., Ringland, R. R., and S. Craig.  
*Development of Handling Quality Criteria for Aircraft with Independent Control of Six Degrees of Freedom.* TR-81-3027. Air Force Wright Aeronautical Laboratories, Ohio. April 1981.
- 7) Tischler, M. B. *Digital Control of Highly Augmented Combat Rotorcraft.* NASA-TM 88346 and USAAVSCOM TR 87-A-5. Ames Research Center, Moffett Field. May 1987.
- 8) Horowitz, I. "Survey of Quantitative Feedback Theory (QFT)." *International Journal of Control.* Vol. 53, No. 2, pp. 255-291. 1991.
- 9) Houppis, C. H. *Quantitative Feedback Theory (QFT): Technique for Designing Multivariable Control Systems.* AFWAL-TR-86-3107. Air Force Wright Aeronautical Laboratories, Wright-Patterson AFB, Ohio. January 1987.
- 10) Horowitz, I. *Quantitative Feedback Design Theory (QFT).* QFT Publications, Boulder, Colorado. 1992
- 11) Kim, F. D., Celi, R. Tischler, M. B. *Higher-Order State-Space Simulation Models of Helicopter Flight Mechanics.* 16th European Rotorcraft Forum. Glasgow, UK. September 1990.
- 12) Howlett, J. J. *UH-60A Black Hawk Engineering Simulation Program: Volume I -- Mathematical Model.* NASA CR-166309. 1981.

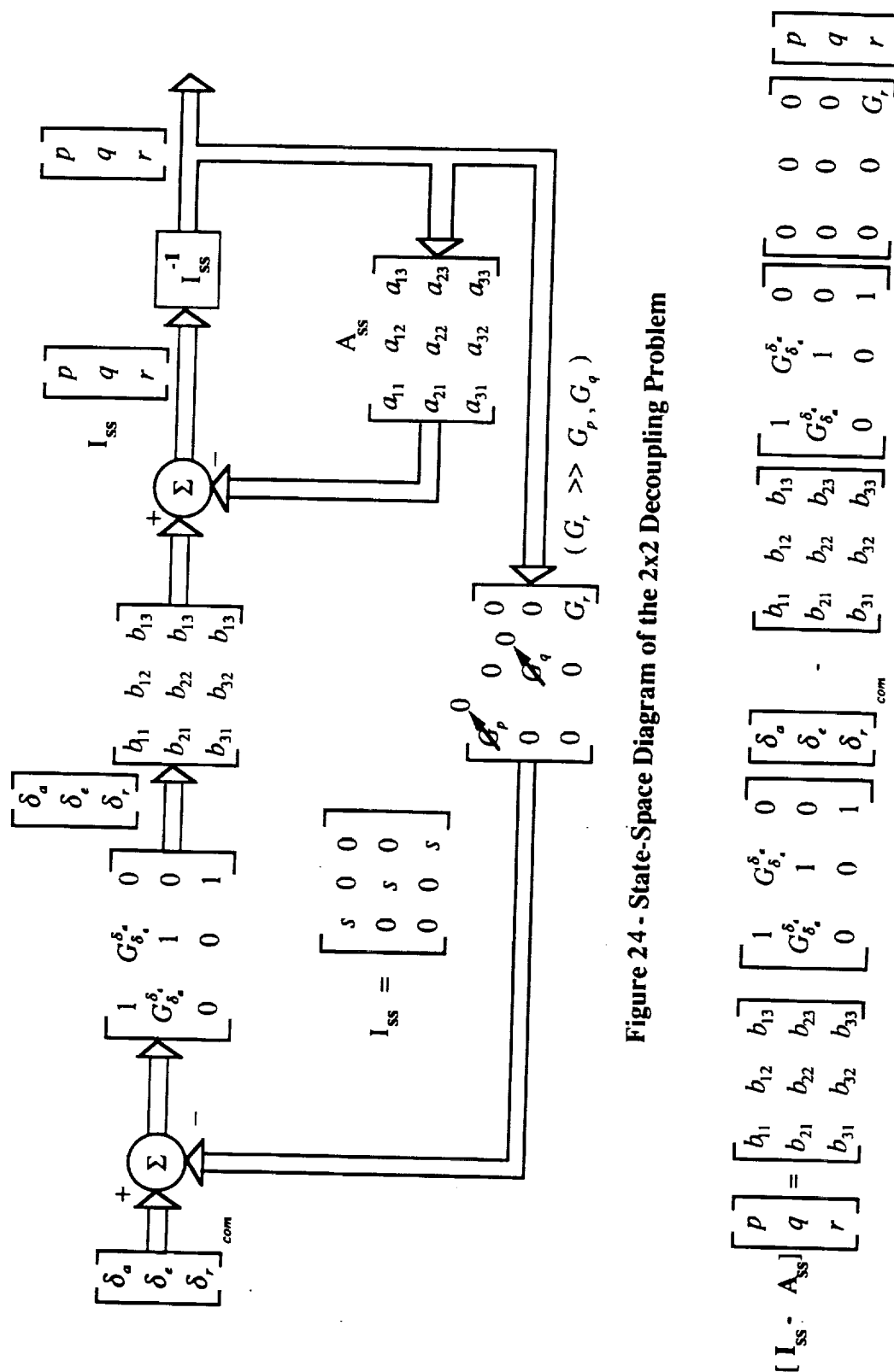
- 13) Landis, Kenneth H. and Glusman, Steven I. *Development of ADOCS Controllers and Control Laws*. NASA CR-177339. 1985.
- 14) Lee, Eugene A. "LCAP2 - Linear Controls Analysis Program." *IEEE Control Systems Magazine*. Vol. 2, No. 4, pp. 15-18. December 1982.
- 15) Hodgkinson, J., and Buckley, J. *NAVFIT - General Purpose Frequency Response Curve Fit Program (Arbitrary Order)*. October 1978.
- 16) Tischler, M. B. *Frequency-Response Identification of XV-15 Tilt-Rotor Aircraft Dynamics*. NASA TM 89428, ARMY TM 87-A-2. May 1987.
- 17) Rousseeuw, Peter J. and Leroy, Annick M. *Robust Regression and Outlier Detection*. John Wiley and Sons, Inc. New York. 1987.

## **APPENDIX A**

### **DERIVATION OF COUPLING NUMERATORS FOR PITCH-ROLL COUPLING**

This appendix contains a derivation of an ideal crossfeed for the 2x2 decoupling problem shown in Figure 3. The main objective of this derivation is to show the transition of a state space model to classical coupling numerators.

The state-space diagram in Figure 24 is equivalent to the classical block diagram in Figure 3. However, matrices shown in the state-space diagram may contain elements of transfer functions. This allows the matrix of crossfeeds to contain transfer functions. Only three states and three controls are shown in this derivation in contrast to the eight states used in the actual analysis. Therefore, the results remain in symbolic form without a sample numeric calculation.



$$[I_{ss} - A_{ss}] = A_s = \begin{bmatrix} a_{s11} & a_{s12} & a_{s13} \\ a_{s21} & a_{s22} & a_{s23} \\ a_{s31} & a_{s32} & a_{s33} \end{bmatrix}$$

$$\begin{bmatrix} a_{s11} & a_{s12} & a_{s13} + b_{13}G_r \\ a_{s21} & a_{s22} & a_{s23} + b_{23}G_r \\ a_{s31} & a_{s32} & a_{s33} + b_{33}G_r \end{bmatrix} \begin{bmatrix} p \\ q \\ r \end{bmatrix} = \begin{bmatrix} b_{11} + b_{12}G_{\delta_s}^{\delta_s} & b_{12} + b_{11}G_{\delta_s}^{\delta_s} & b_{13} \\ b_{21} + b_{22}G_{\delta_s}^{\delta_s} & b_{22} + b_{21}G_{\delta_s}^{\delta_s} & b_{23} \\ b_{31} + b_{32}G_{\delta_s}^{\delta_s} & b_{32} + b_{31}G_{\delta_s}^{\delta_s} & b_{33} \end{bmatrix} \begin{bmatrix} \delta_a \\ \delta_s \\ \delta_r \end{bmatrix}_{com}$$

Solve for  $\left. \frac{q}{\delta_a} \right|_{\delta_r}$

$$\left. \frac{q}{\delta_a} \right|_{\delta_r} = \frac{\begin{vmatrix} a_{s11} & b_{11} + b_{12}G_{\delta_s}^{\delta_s} & a_{s13} + b_{13}G_r \\ a_{s21} & b_{21} + b_{22}G_{\delta_s}^{\delta_s} & a_{s23} + b_{23}G_r \\ a_{s31} & b_{31} + b_{32}G_{\delta_s}^{\delta_s} & a_{s33} + b_{33}G_r \end{vmatrix}}{\begin{vmatrix} a_{s11} & a_{s12} & a_{s13} + b_{13}G_r \\ a_{s21} & a_{s22} & a_{s23} + b_{23}G_r \\ a_{s31} & a_{s32} & a_{s33} + b_{33}G_r \end{vmatrix}}} = \frac{N}{D}$$

Solve for the numerator, N

$$N = \begin{vmatrix} a_{s1} & b_{11} + b_{12}G_{\delta_s}^{\delta_r} & a_{s3} + b_{13}G_r \\ a_{s21} & b_{21} + b_{22}G_{\delta_s}^{\delta_r} & a_{s23} + b_{23}G_r \\ a_{s31} & b_{31} + b_{32}G_{\delta_s}^{\delta_r} & a_{s33} + b_{33}G_r \end{vmatrix} = \begin{vmatrix} a_{s1} & b_1 + b_2G_{\delta_s}^{\delta_r} & a_{s3} + b_3G_r \end{vmatrix} =$$

( numerator matrix described in one row  
retaining column subscript notation )

$$\begin{vmatrix} a_{s1} & b_1 & a_{s3} + b_3G_r \end{vmatrix} + \begin{vmatrix} a_{s1} & b_2G_{\delta_s}^{\delta_r} & a_{s3} + b_3G_r \end{vmatrix} =$$

$$\begin{vmatrix} a_{s1} & b_1 & a_{s3} \end{vmatrix} + \begin{vmatrix} a_{s1} & b_1 & b_3G_r \end{vmatrix} + \begin{vmatrix} a_{s1} & b_2G_{\delta_s}^{\delta_r} & a_{s3} \end{vmatrix} + \begin{vmatrix} a_{s1} & b_2G_{\delta_s}^{\delta_r} & b_3G_r \end{vmatrix} =$$

$$N_{\delta_s}^q + G_r N_{\delta_s \delta_r}^{q,r} + G_{\delta_s}^{\delta_r} N_{\delta_s}^q + G_{\delta_s}^{\delta_r} G_r N_{\delta_s \delta_r}^{q,r} \equiv G_r N_{\delta_s \delta_r}^{q,r} + G_{\delta_s}^{\delta_r} G_r N_{\delta_s \delta_r}^{q,r},$$

( large Gr assumption)

For decoupling, it is desired that  $\left. \frac{q}{\delta_{s1\delta_r}} \right|' = 0$

$$N = N_{\delta_s \delta_r}^{q,r} + G_{\delta_s}^{\delta_r} N_{\delta_s \delta_r}^{q,r} = 0$$

$$\therefore G_{\delta_s \delta_r}^{\delta_r} = \frac{-N_{\delta_s \delta_r}^{q,r}}{N_{\delta_s \delta_r}^{q,r}}$$

## APPENDIX B

### CONFIGURATION MATRICES

Linearized flight dynamics are commonly described with the state equation:

$$\dot{\bar{\mathbf{x}}} = \mathbf{A}\bar{\mathbf{x}} + \mathbf{B}\bar{\mathbf{u}}$$

The state vector is defined in UMGENHEL as:

$$\bar{\mathbf{x}} = [u(ft/s) \quad v(ft/s) \quad w(ft/s) \quad p(rad/s) \quad q(rad/s) \quad r(rad/s) \quad \phi(rad) \quad \theta(rad)]^T$$

The control vector is defined as:

$$\bar{\mathbf{u}} = [\delta_a(in) \quad \delta_e(in) \quad \delta_c(in) \quad \delta_r(in)]^T$$

The state matrix,  $\mathbf{A}$ , and the control matrix,  $\mathbf{B}$ , are listed for each of the 25 flight conditions. The flight conditions are categorized into groups of occurrence probability.

#### ***Group I: Most Probable***

##### ***Flight Condition 1: 1 Knot Forward***

$$\mathbf{A} = \begin{bmatrix} -0.01 & -0.01 & 0.01 & -1.0 & 0.99 & -0.27 & 0.0 & -32.0 \\ 0.0 & -0.05 & 0.0 & -0.35 & -0.74 & -1.3 & 32.0 & 0.1 \\ 0.03 & 0.0 & -0.26 & -0.1 & 1.5 & 2.1 & 1.5 & -2.2 \\ 0.03 & -0.04 & 0.0 & -3.7 & -1.3 & 0.04 & 0.0 & 0.0 \\ 0.01 & 0.01 & 0.0 & 0.18 & -0.69 & -0.09 & 0.0 & 0.0 \\ 0.0 & 0.0 & 0.0 & -0.17 & -0.09 & -0.22 & 0.0 & 0.0 \\ 0.0 & 0.0 & 0.0 & 1.0 & 0.0 & 0.07 & 0.0 & 0.0 \\ 0.0 & 0.0 & 0.0 & 0.0 & 1.0 & 0.05 & 0.0 & 0.0 \end{bmatrix}$$

$$\mathbf{B} = \begin{bmatrix} -0.06 & -1.2 & 0.7 & 0.72 \\ 0.41 & -0.07 & 0.12 & -0.91 \\ 0.01 & -0.02 & -7.0 & 0.39 \\ 1.1 & 0.06 & -0.12 & -0.5 \\ 0.01 & 0.29 & -0.02 & -0.02 \\ 0.06 & 0.0 & 0.07 & 0.38 \\ 0.0 & 0.0 & 0.0 & 0.0 \\ 0.0 & 0.0 & 0.0 & 0.0 \end{bmatrix}$$



**Group 1: Most Probable (continued)****Flight Condition 2: 15 Knots Forward**

$$A = \begin{bmatrix} -0.01 & 0.0 & 0.03 & -0.82 & -2.1 & -0.37 & 0.0 & -32.0 \\ 0.0 & -0.07 & -0.02 & 2.0 & -0.71 & -24.0 & 32.0 & 0.1 \\ -0.1 & 0.0 & -0.29 & 0.48 & 26.0 & 1.7 & 1.1 & -3.1 \\ 0.02 & -0.03 & 0.02 & -4.0 & -1.2 & 0.13 & 0.0 & 0.0 \\ 0.01 & 0.01 & 0.01 & 0.13 & -0.69 & -0.13 & 0.0 & 0.0 \\ 0.0 & 0.01 & 0.0 & -0.26 & 0.03 & -0.49 & 0.0 & 0.0 \\ 0.0 & 0.0 & 0.0 & 1.0 & 0.0 & 0.1 & 0.0 & 0.0 \\ 0.0 & 0.0 & 0.0 & 0.0 & 1.0 & 0.03 & 0.0 & 0.0 \end{bmatrix}$$

$$B = \begin{bmatrix} -0.08 & -1.0 & 0.9 & 0.65 \\ 0.39 & -0.08 & 0.12 & -0.97 \\ 0.12 & -0.51 & -6.5 & 0.7 \\ 1.1 & 0.05 & -0.09 & -0.53 \\ 0.01 & 0.27 & 0.0 & 0.0 \\ 0.06 & -0.03 & 0.06 & 0.41 \\ 0.0 & 0.0 & 0.0 & 0.0 \\ 0.0 & 0.0 & 0.0 & 0.0 \end{bmatrix}$$
**Flight Condition 3: 15 Knots Rearward**

$$A = \begin{bmatrix} -0.04 & 0.01 & 0.02 & -0.9 & 3.1 & -0.25 & 0.0 & -32.0 \\ -0.01 & -0.02 & -0.01 & -2.5 & -0.51 & 26.0 & 32.0 & 0.1 \\ 0.16 & 0.0 & -0.3 & 0.86 & -27.0 & 1.9 & 1.1 & -2.8 \\ -0.03 & -0.01 & 0.02 & -3.9 & -0.54 & -0.03 & 0.0 & 0.0 \\ 0.0 & 0.0 & 0.0 & 0.1 & -0.65 & -0.11 & 0.0 & 0.0 \\ 0.0 & 0.0 & 0.0 & -0.27 & -0.06 & -0.22 & 0.0 & 0.0 \\ 0.0 & 0.0 & 0.0 & 1.0 & 0.0 & 0.09 & 0.0 & 0.0 \\ 0.0 & 0.0 & 0.0 & 0.0 & 1.0 & 0.03 & 0.0 & 0.0 \end{bmatrix}$$

$$B = \begin{bmatrix} -0.07 & -1.2 & 0.84 & 0.72 \\ 0.4 & -0.09 & 0.16 & -0.91 \\ 0.08 & 0.69 & -6.8 & -0.01 \\ 1.0 & -0.07 & -0.07 & -0.42 \\ 0.01 & 0.27 & -0.03 & -0.01 \\ 0.06 & -0.02 & 0.06 & 0.39 \\ 0.0 & 0.0 & 0.0 & 0.0 \\ 0.0 & 0.0 & 0.0 & 0.0 \end{bmatrix}$$
**Flight Condition 7: 15 Knots,  $\beta = 80$  deg.**

$$A = \begin{bmatrix} -0.01 & 0.04 & 0.06 & -0.68 & -3.5 & 25.0 & 0.0 & -32.0 \\ -0.02 & -0.09 & 0.01 & 4.1 & -0.51 & -3.8 & 32.0 & 0.0 \\ 0.01 & -0.16 & -0.29 & -26.0 & 4.1 & 1.1 & -0.04 & -2.2 \\ 0.01 & -0.02 & 0.0 & -4.0 & -0.81 & -0.02 & 0.0 & 0.0 \\ 0.02 & 0.01 & 0.0 & 0.15 & -0.91 & -0.14 & 0.0 & 0.0 \\ 0.0 & 0.01 & 0.0 & -0.17 & -0.08 & -0.35 & 0.0 & 0.0 \\ 0.0 & 0.0 & 0.0 & 1.0 & 0.0 & 0.07 & 0.0 & 0.02 \\ 0.0 & 0.0 & 0.0 & 0.0 & 1.0 & 0.0 & -0.02 & 0.0 \end{bmatrix}$$

$$B = \begin{bmatrix} -0.06 & -0.97 & 0.74 & 0.61 \\ 0.32 & -0.05 & 0.07 & -0.93 \\ 0.32 & 0.04 & -6.5 & 0.37 \\ 0.99 & 0.04 & -0.19 & -0.49 \\ 0.0 & 0.28 & -0.03 & -0.02 \\ 0.06 & -0.03 & 0.02 & 0.4 \\ 0.0 & 0.0 & 0.0 & 0.0 \\ 0.0 & 0.0 & 0.0 & 0.0 \end{bmatrix}$$
**Flight Condition 9: 15 Knots,  $\beta = -80$  deg.**

$$A = \begin{bmatrix} 0.0 & 0.01 & 0.05 & -0.91 & -4.6 & -25.0 & 0.0 & -32.0 \\ -0.02 & -0.08 & 0.0 & 5.2 & -0.69 & -3.0 & 32.0 & 0.1 \\ 0.0 & 0.15 & -0.29 & 26.0 & 3.7 & 1.9 & 1.9 & -1.7 \\ 0.01 & -0.01 & 0.0 & -3.9 & -0.9 & -0.05 & 0.0 & 0.0 \\ 0.01 & 0.0 & 0.0 & 0.13 & -0.72 & -0.04 & 0.0 & 0.0 \\ 0.0 & 0.01 & 0.0 & -0.17 & 0.07 & -0.34 & 0.0 & 0.0 \\ 0.0 & 0.0 & 0.0 & 1.0 & 0.0 & 0.05 & 0.0 & 0.02 \\ 0.0 & 0.0 & 0.0 & 0.0 & 1.0 & 0.06 & -0.02 & 0.0 \end{bmatrix}$$

$$B = \begin{bmatrix} -0.01 & -0.97 & 0.68 & 0.61 \\ 0.32 & -0.05 & 0.26 & -0.85 \\ -0.3 & -0.15 & -6.4 & 0.45 \\ 0.99 & 0.01 & 0.04 & -0.44 \\ 0.01 & 0.26 & -0.02 & -0.01 \\ 0.05 & -0.02 & 0.05 & 0.36 \\ 0.0 & 0.0 & 0.0 & 0.0 \\ 0.0 & 0.0 & 0.0 & 0.0 \end{bmatrix}$$

**Group II: Less Probable****Flight Condition 6: 15 Knots.  $\beta = 45$  deg.**

$$A = \begin{bmatrix} 0.0 & 0.02 & 0.05 & -0.87 & -2.7 & 17.0 & 0.0 & -32.0 \\ 0.0 & -0.1 & -0.03 & 3.1 & -0.48 & -17.0 & 32.0 & 0.06 \\ -0.08 & -0.09 & -0.29 & -18.0 & 19.0 & 1.5 & 0.61 & -2.9 \\ 0.03 & -0.03 & 0.01 & -4.1 & -0.93 & 0.07 & 0.0 & 0.0 \\ 0.01 & 0.01 & 0.01 & 0.16 & -0.71 & -0.12 & 0.0 & 0.0 \\ 0.0 & 0.02 & 0.0 & -0.25 & -0.06 & -0.48 & 0.0 & 0.0 \\ 0.0 & 0.0 & 0.0 & 1.0 & 0.0 & 0.09 & 0.0 & 0.01 \\ 0.0 & 0.0 & 0.0 & 0.0 & 1.0 & 0.02 & -0.01 & 0.0 \end{bmatrix}$$

$$B = \begin{bmatrix} -0.07 & -1.1 & 0.85 & 0.67 \\ 0.36 & -0.1 & 0.08 & -0.96 \\ 0.27 & -0.25 & -6.5 & 0.56 \\ 1.0 & 0.0 & -0.15 & -0.5 \\ 0.0 & 0.26 & -0.01 & 0.0 \\ 0.06 & -0.03 & 0.04 & 0.41 \\ 0.0 & 0.0 & 0.0 & 0.0 \\ 0.0 & 0.0 & 0.0 & 0.0 \end{bmatrix}$$
**Flight Condition 8: 15 Knots.  $\beta = -45$  deg.**

$$A = \begin{bmatrix} 0.01 & 0.0 & 0.03 & -1.0 & -2.4 & -19.0 & 0.0 & -32.0 \\ -0.01 & -0.09 & -0.03 & 2.7 & -0.63 & -17.0 & 32.0 & 0.23 \\ -0.06 & 0.13 & -0.3 & 19.0 & 18.0 & 1.7 & 2.7 & -2.7 \\ 0.02 & -0.01 & 0.01 & -3.9 & -0.98 & 0.13 & 0.0 & 0.0 \\ 0.01 & 0.0 & 0.0 & 0.14 & -0.63 & -0.16 & 0.0 & 0.0 \\ 0.0 & 0.02 & 0.0 & -0.17 & 0.12 & -0.48 & 0.0 & 0.0 \\ 0.0 & 0.0 & 0.0 & 1.0 & -0.01 & 0.09 & 0.0 & 0.0 \\ 0.0 & 0.0 & 0.0 & 0.0 & 1.0 & 0.08 & 0.0 & 0.0 \end{bmatrix}$$

$$B = \begin{bmatrix} -0.01 & -1.0 & 0.75 & 0.63 \\ 0.34 & -0.09 & 0.22 & -0.89 \\ -0.08 & -0.55 & -6.4 & 0.69 \\ 1.0 & -0.02 & -0.01 & -0.45 \\ 0.01 & 0.25 & -0.01 & 0.01 \\ 0.05 & -0.02 & 0.06 & 0.39 \\ 0.0 & 0.0 & 0.0 & 0.0 \\ 0.0 & 0.0 & 0.0 & 0.0 \end{bmatrix}$$
**Flight Condition 14: 6 Knots.  $\gamma = 80$  deg.**

$$A = \begin{bmatrix} -0.03 & 0.0 & 0.01 & -1.2 & 12.0 & -0.3 & 0.0 & -32.0 \\ -0.01 & -0.04 & -0.01 & -11.0 & -0.87 & 1.4 & 32.0 & 0.11 \\ 0.03 & 0.0 & -0.31 & -0.11 & -1.1 & 2.6 & 1.9 & -1.9 \\ -0.03 & -0.02 & 0.0 & -3.8 & -1.0 & 0.08 & 0.0 & 0.0 \\ 0.0 & 0.0 & 0.0 & 0.19 & -0.66 & -0.11 & 0.0 & 0.0 \\ 0.0 & 0.0 & 0.0 & -0.19 & -0.05 & -0.26 & 0.0 & 0.0 \\ 0.0 & 0.0 & 0.0 & 1.0 & 0.0 & 0.06 & 0.0 & 0.0 \\ 0.0 & 0.0 & 0.0 & 0.0 & 1.0 & 0.06 & 0.0 & 0.0 \end{bmatrix}$$

$$B = \begin{bmatrix} -0.11 & -1.4 & 0.73 & 0.87 \\ 0.53 & -0.15 & 0.1 & -0.92 \\ 0.0 & 0.05 & -7.2 & 0.38 \\ 1.2 & -0.09 & -0.12 & -0.44 \\ 0.01 & 0.31 & -0.02 & -0.03 \\ 0.06 & -0.01 & 0.11 & 0.41 \\ 0.0 & 0.0 & 0.0 & 0.0 \\ 0.0 & 0.0 & 0.0 & 0.0 \end{bmatrix}$$
**Flight Condition 15: 6 Knots.  $\gamma = -70$  deg.**

$$A = \begin{bmatrix} 0.0 & 0.0 & 0.01 & -1.0 & -8.1 & -0.28 & 0.0 & -32.0 \\ 0.0 & -0.05 & 0.0 & 8.7 & -0.79 & -2.3 & 32.0 & 0.1 \\ 0.02 & 0.0 & -0.24 & -0.04 & 2.6 & 2.1 & 1.4 & -2.3 \\ 0.04 & -0.03 & 0.0 & -3.8 & -1.4 & 0.05 & 0.0 & 0.0 \\ 0.01 & 0.0 & 0.0 & 0.16 & -0.68 & -0.09 & 0.0 & 0.0 \\ 0.0 & 0.0 & 0.0 & -0.19 & -0.07 & -0.22 & 0.0 & 0.0 \\ 0.0 & 0.0 & 0.0 & 1.0 & 0.0 & 0.07 & 0.0 & 0.0 \\ 0.0 & 0.0 & 0.0 & 0.0 & 1.0 & 0.04 & 0.0 & 0.0 \end{bmatrix}$$

$$B = \begin{bmatrix} -0.06 & -1.2 & 0.72 & 0.74 \\ 0.43 & -0.06 & 0.11 & -0.91 \\ 0.01 & -0.05 & -7.0 & 0.41 \\ 1.1 & 0.07 & -0.13 & -0.5 \\ 0.01 & 0.29 & -0.02 & -0.02 \\ 0.06 & -0.01 & 0.07 & 0.39 \\ 0.0 & 0.0 & 0.0 & 0.0 \\ 0.0 & 0.0 & 0.0 & 0.0 \end{bmatrix}$$

**Group III: Least Probable****Flight Condition 4: 30 Knots Forward**

$$A = \begin{bmatrix} -0.04 & 0.0 & 0.01 & -0.71 & -1.1 & -0.29 & 0.0 & -32.0 \\ 0.0 & -0.07 & 0.0 & 1.4 & -0.65 & -49.0 & 32.0 & 0.03 \\ -0.17 & -0.01 & -0.43 & 1.9 & 51.0 & 1.6 & 0.69 & -1.3 \\ 0.0 & -0.03 & 0.03 & -3.7 & -1.0 & 0.28 & 0.0 & 0.0 \\ -0.01 & 0.01 & 0.0 & 0.15 & -0.93 & -0.16 & 0.0 & 0.0 \\ 0.0 & 0.01 & 0.0 & -0.22 & -0.04 & -0.53 & 0.0 & 0.0 \\ 0.0 & 0.0 & 0.0 & 1.0 & 0.0 & 0.04 & 0.0 & 0.0 \\ 0.0 & 0.0 & 0.0 & 0.0 & 1.0 & 0.02 & 0.0 & 0.0 \end{bmatrix}$$

$$B = \begin{bmatrix} -0.07 & -1.0 & 0.6 & 0.66 \\ 0.4 & -0.06 & 0.14 & -1.1 \\ 0.28 & -0.88 & -6.4 & 0.97 \\ 1.1 & 0.08 & 0.02 & -0.61 \\ 0.01 & 0.29 & 0.04 & 0.02 \\ 0.05 & -0.01 & 0.03 & 0.46 \\ 0.0 & 0.0 & 0.0 & 0.0 \\ 0.0 & 0.0 & 0.0 & 0.0 \end{bmatrix}$$
**Flight Condition 5: 30 Knots,  $\beta = 180$  deg.**

$$A = \begin{bmatrix} -0.05 & 0.01 & 0.04 & -0.96 & 7.7 & -0.3 & 0.0 & -32.0 \\ 0.0 & -0.02 & 0.0 & -6.7 & -0.57 & 51.0 & 32.0 & 0.09 \\ 0.19 & -0.02 & -0.4 & 2.4 & -52.0 & 1.9 & 0.77 & -3.7 \\ -0.01 & -0.01 & 0.03 & -3.9 & -0.72 & -0.05 & 0.0 & 0.0 \\ 0.0 & 0.0 & 0.0 & 0.08 & -0.76 & -0.12 & 0.0 & 0.0 \\ 0.0 & 0.01 & 0.0 & -0.31 & -0.11 & -0.26 & 0.0 & 0.0 \\ 0.0 & 0.0 & 0.0 & 1.0 & 0.0 & 0.12 & 0.0 & 0.0 \\ 0.0 & 0.0 & 0.0 & 0.0 & 1.0 & 0.02 & 0.0 & 0.0 \end{bmatrix}$$

$$B = \begin{bmatrix} -0.12 & -1.3 & 1.1 & 0.79 \\ 0.42 & -0.07 & 0.19 & -1.0 \\ 0.16 & 1.4 & -7.0 & -0.36 \\ 1.1 & -0.04 & -0.01 & -0.48 \\ 0.02 & 0.26 & -0.06 & 0.01 \\ 0.06 & -0.03 & 0.03 & 0.42 \\ 0.0 & 0.0 & 0.0 & 0.0 \\ 0.0 & 0.0 & 0.0 & 0.0 \end{bmatrix}$$
**Flight Condition 10: 30 Knots,  $\beta = 45$  deg.**

$$A = \begin{bmatrix} -0.05 & 0.01 & 0.0 & -0.88 & -0.87 & 35.0 & 0.0 & -32.0 \\ 0.0 & -0.1 & 0.0 & 0.97 & -0.36 & -35.0 & 32.0 & -0.07 \\ -0.12 & -0.12 & -0.44 & -35.0 & 37.0 & 1.4 & -0.92 & -2.5 \\ 0.02 & -0.03 & 0.01 & -4.1 & -0.74 & 0.2 & 0.0 & 0.0 \\ -0.01 & 0.0 & 0.0 & 0.2 & -0.88 & -0.15 & 0.0 & 0.0 \\ 0.0 & 0.01 & 0.0 & -0.24 & -0.16 & -0.47 & 0.0 & 0.0 \\ 0.0 & 0.0 & 0.0 & 1.0 & 0.0 & 0.08 & 0.0 & 0.0 \\ 0.0 & 0.0 & 0.0 & 0.0 & 1.0 & -0.03 & 0.0 & 0.0 \end{bmatrix}$$

$$B = \begin{bmatrix} -0.11 & -1.1 & 0.84 & 0.69 \\ 0.42 & -0.1 & -0.07 & -1.1 \\ 0.54 & -0.34 & -6.5 & 0.7 \\ 1.0 & 0.06 & -0.16 & -0.63 \\ 0.0 & 0.3 & 0.04 & 0.01 \\ 0.06 & -0.02 & 0.02 & 0.49 \\ 0.0 & 0.0 & 0.0 & 0.0 \\ 0.0 & 0.0 & 0.0 & 0.0 \end{bmatrix}$$
**Flight Condition 11: 30 Knots,  $\beta = 80$  deg.**

$$A = \begin{bmatrix} -0.06 & 0.03 & 0.04 & -0.88 & 3.8 & 49.0 & 0.0 & -32.0 \\ -0.01 & -0.13 & 0.01 & -2.7 & -0.49 & -7.2 & 32.0 & -0.21 \\ 0.12 & -0.15 & -0.4 & -51.0 & 7.6 & 1.2 & -1.9 & -3.4 \\ 0.01 & -0.02 & 0.0 & -4.0 & -0.93 & 0.01 & 0.0 & 0.0 \\ 0.04 & 0.01 & 0.01 & 0.19 & -1.2 & -0.19 & 0.0 & 0.0 \\ 0.01 & 0.01 & 0.0 & -0.23 & -0.21 & -0.53 & 0.0 & 0.0 \\ 0.0 & 0.0 & 0.0 & 1.0 & 0.01 & 0.11 & 0.0 & 0.0 \\ 0.0 & 0.0 & 0.0 & 0.0 & 1.0 & -0.06 & 0.0 & 0.0 \end{bmatrix}$$

$$B = \begin{bmatrix} -0.11 & -1.2 & 0.92 & 0.74 \\ 0.43 & -0.11 & -0.01 & -1.1 \\ 0.64 & 0.07 & -6.9 & 0.43 \\ 1.1 & 0.02 & -0.24 & -0.6 \\ 0.0 & 0.32 & -0.05 & -0.01 \\ 0.06 & -0.01 & 0.0 & 0.47 \\ 0.0 & 0.0 & 0.0 & 0.0 \\ 0.0 & 0.0 & 0.0 & 0.0 \end{bmatrix}$$

**Group III: Least Probable (continued)****Flight Condition 12: 30 Knots,  $\beta = -45$  deg.**

$$A = \begin{bmatrix} -0.05 & 0.0 & 0.01 & -0.67 & 1.3 & -36.0 & 0.0 & -32.0 \\ 0.01 & -0.1 & 0.0 & -1.3 & -0.76 & -35.0 & 32.0 & 0.19 \\ -0.12 & 0.11 & -0.42 & 37.0 & 35.0 & 1.8 & 2.8 & -2.2 \\ 0.01 & -0.01 & 0.02 & -4.1 & -0.95 & 0.19 & 0.0 & 0.0 \\ -0.01 & 0.01 & 0.0 & 0.13 & -0.84 & -0.17 & 0.0 & 0.0 \\ 0.0 & 0.02 & 0.0 & -0.19 & 0.13 & -0.48 & 0.0 & 0.0 \\ 0.0 & 0.0 & 0.0 & 1.0 & -0.01 & 0.07 & 0.0 & 0.0 \\ 0.0 & 0.0 & 0.0 & 0.0 & 1.0 & 0.09 & 0.0 & 0.0 \end{bmatrix}$$

$$B = \begin{bmatrix} 0.0 & -1.0 & 0.83 & 0.66 \\ 0.4 & -0.12 & 0.37 & -1.0 \\ -0.23 & -0.95 & -6.4 & 0.97 \\ 1.1 & -0.07 & 0.13 & -0.49 \\ 0.01 & 0.29 & 0.04 & 0.01 \\ 0.06 & -0.02 & 0.04 & 0.44 \\ 0.0 & 0.0 & 0.0 & 0.0 \\ 0.0 & 0.0 & 0.0 & 0.0 \end{bmatrix}$$
**Flight Condition 13: 30 Knots,  $\beta = -80$  deg.**

$$A = \begin{bmatrix} 0.0 & -0.02 & 0.04 & -0.96 & 7.4 & -50.0 & 0.0 & -32.0 \\ 0.02 & -0.13 & -0.01 & -6.7 & -1.1 & -4.9 & 32.0 & 0.4 \\ 0.06 & 0.14 & -0.41 & 51.0 & 6.1 & 2.1 & 4.4 & -2.9 \\ 0.01 & -0.01 & 0.0 & -3.9 & -0.99 & 0.04 & 0.0 & 0.0 \\ 0.01 & 0.0 & 0.0 & 0.14 & -0.77 & -0.07 & 0.0 & 0.0 \\ -0.01 & 0.02 & 0.0 & -0.16 & 0.26 & -0.54 & 0.0 & 0.0 \\ 0.0 & 0.0 & 0.0 & 1.0 & -0.01 & 0.09 & 0.0 & 0.0 \\ 0.0 & 0.0 & 0.0 & 0.0 & 0.99 & 0.14 & 0.0 & 0.0 \end{bmatrix}$$

$$B = \begin{bmatrix} 0.01 & -1.1 & 0.78 & 0.68 \\ 0.39 & -0.07 & 0.41 & -0.77 \\ -0.64 & -0.25 & -6.7 & 0.47 \\ 1.0 & -0.04 & 0.16 & -0.37 \\ 0.01 & 0.29 & -0.03 & -0.04 \\ 0.06 & -0.04 & 0.09 & 0.34 \\ 0.0 & 0.0 & 0.0 & 0.0 \\ 0.0 & 0.0 & 0.0 & 0.0 \end{bmatrix}$$
**Flight Condition 16: 12 Knots,  $\gamma = 80$  deg.**

$$A = \begin{bmatrix} -0.02 & 0.02 & -0.01 & -1.3 & 23.0 & -0.32 & 0.0 & -32.0 \\ -0.01 & -0.07 & -0.02 & -23.0 & -0.89 & -4.3 & 32.0 & 0.16 \\ 0.05 & 0.01 & -0.34 & -0.12 & 4.6 & 2.8 & 2.2 & -2.4 \\ 0.02 & -0.05 & 0.0 & -3.7 & -1.6 & 0.17 & 0.0 & 0.0 \\ 0.01 & 0.0 & 0.0 & 0.24 & -0.77 & -0.12 & 0.0 & 0.0 \\ 0.0 & 0.0 & 0.0 & -0.19 & -0.03 & -0.3 & 0.0 & 0.0 \\ 0.0 & 0.0 & 0.0 & 1.0 & -0.01 & 0.07 & 0.0 & 0.01 \\ 0.0 & 0.0 & 0.0 & 0.0 & 1.0 & 0.07 & -0.01 & 0.0 \end{bmatrix}$$

$$B = \begin{bmatrix} -0.13 & -1.5 & 0.78 & 0.89 \\ 0.55 & -0.19 & 0.06 & -0.94 \\ 0.01 & -0.03 & -7.1 & 0.43 \\ 1.2 & -0.02 & -0.16 & -0.5 \\ 0.01 & 0.33 & -0.03 & -0.03 \\ 0.06 & -0.01 & 0.16 & 0.43 \\ 0.0 & 0.0 & 0.0 & 0.0 \\ 0.0 & 0.0 & 0.0 & 0.0 \end{bmatrix}$$
**Flight Condition 17: 45 Knots,  $\gamma = -7.06$  deg.,  $\phi = 20$  deg.**

$$A = \begin{bmatrix} -0.05 & 0.27 & -0.24 & -1.0 & -3.6 & 4.8 & 0.0 & -32.0 \\ -0.27 & -0.09 & 0.01 & 4.8 & -0.78 & -74.0 & 25.0 & 0.38 \\ 0.06 & -0.02 & -0.5 & -2.8 & 77.0 & 2.0 & -20.0 & 0.46 \\ 0.0 & -0.03 & 0.03 & -3.8 & -1.2 & 0.41 & 0.0 & 0.0 \\ 0.0 & 0.01 & 0.0 & 0.33 & -0.73 & -0.16 & 0.0 & 0.0 \\ -0.01 & 0.01 & -0.01 & -0.38 & 0.03 & -0.6 & 0.0 & 0.0 \\ 0.0 & 0.0 & 0.0 & 1.0 & -0.01 & -0.01 & 0.0 & 0.35 \\ 0.0 & 0.0 & 0.0 & 0.0 & 0.77 & -0.63 & -0.35 & 0.0 \end{bmatrix}$$

$$B = \begin{bmatrix} -0.1 & -1.5 & 0.15 & 0.92 \\ 0.55 & -0.08 & 0.03 & -1.1 \\ 0.38 & -1.6 & -6.8 & 1.4 \\ 1.2 & 0.17 & -0.01 & -0.67 \\ 0.0 & 0.29 & 0.0 & 0.03 \\ 0.06 & 0.02 & 0.02 & 0.46 \\ 0.0 & 0.0 & 0.0 & 0.0 \\ 0.0 & 0.0 & 0.0 & 0.0 \end{bmatrix}$$

**Group III: Least Probable (continued)****Flight Condition 18: 45 Knots.  $\gamma = -7.06$  deg.,  $\phi = -20$  deg.**

$$A = \begin{bmatrix} -0.05 & -0.27 & -0.23 & -1.1 & -3.6 & 2.6 & 0.0 & -32.0 \\ 0.27 & -0.08 & -0.03 & 4.5 & -1.1 & -74.0 & 25.0 & -1.8 \\ 0.05 & 0.02 & -0.51 & -0.51 & 77.0 & 2.0 & 20.0 & 2.2 \\ 0.0 & -0.03 & 0.03 & -3.8 & -1.4 & 0.44 & 0.0 & 0.0 \\ 0.0 & 0.01 & 0.0 & -0.14 & -0.73 & -0.2 & 0.0 & 0.0 \\ -0.01 & 0.01 & -0.01 & -0.38 & 0.1 & -0.6 & 0.0 & 0.0 \\ 0.0 & 0.0 & 0.0 & 1.0 & 0.06 & -0.07 & 0.0 & -0.35 \\ 0.0 & 0.0 & 0.0 & 0.0 & 0.78 & 0.63 & 0.35 & 0.0 \end{bmatrix}$$

$$B = \begin{bmatrix} -0.11 & -1.5 & 0.14 & 0.91 \\ 0.56 & -0.06 & 0.05 & -1.2 \\ 0.38 & -1.5 & -7.0 & 1.4 \\ 1.2 & 0.13 & 0.0 & -0.66 \\ 0.01 & 0.3 & 0.01 & 0.02 \\ 0.06 & 0.02 & 0.02 & 0.48 \\ 0.0 & 0.0 & 0.0 & 0.0 \\ 0.0 & 0.0 & 0.0 & 0.0 \end{bmatrix}$$
**Flight Condition 19: 45 Knots.  $\gamma = 7.06$  deg.,  $\phi = 20$  deg.**

$$A = \begin{bmatrix} -0.06 & 0.26 & -0.22 & -1.1 & 11.0 & 16.0 & 0.0 & -32.0 \\ -0.26 & -0.09 & -0.06 & -11.0 & -0.96 & -73.0 & 24.0 & -3.8 \\ 0.07 & 0.03 & -0.5 & -15.0 & 75.0 & 2.5 & -20.0 & -4.6 \\ 0.0 & -0.04 & 0.02 & -3.9 & -1.4 & 0.43 & 0.0 & 0.0 \\ -0.01 & 0.01 & 0.0 & 0.45 & -1.0 & -0.21 & 0.0 & 0.0 \\ 0.0 & 0.0 & 0.0 & -0.44 & 0.05 & -0.58 & 0.0 & 0.0 \\ 0.0 & 0.0 & 0.0 & 1.0 & 0.12 & 0.15 & 0.0 & 0.35 \\ 0.0 & 0.0 & 0.0 & 0.0 & 0.77 & -0.64 & -0.34 & 0.0 \end{bmatrix}$$

$$B = \begin{bmatrix} -0.13 & -1.5 & 0.32 & 0.93 \\ 0.63 & -0.16 & 0.0 & -1.1 \\ 0.43 & -1.5 & -6.8 & 1.3 \\ 1.2 & 0.11 & -0.07 & -0.66 \\ 0.01 & 0.34 & 0.06 & -0.01 \\ 0.06 & 0.02 & 0.06 & 0.47 \\ 0.0 & 0.0 & 0.0 & 0.0 \\ 0.0 & 0.0 & 0.0 & 0.0 \end{bmatrix}$$
**Flight Condition 20: 1 Knot. Main Rotor Speed = 24 rpm**

$$A = \begin{bmatrix} -0.02 & 0.0 & 0.01 & -1.1 & 2.5 & -0.38 & 0.0 & -32.0 \\ 0.0 & -0.05 & 0.0 & -1.8 & -0.76 & -1.2 & 32.0 & 0.12 \\ 0.03 & 0.0 & -0.25 & -0.1 & 1.5 & 2.4 & 1.5 & -2.5 \\ 0.03 & -0.04 & 0.0 & -3.6 & -1.4 & 0.05 & 0.0 & 0.0 \\ 0.01 & 0.0 & 0.0 & 0.18 & -0.66 & -0.09 & 0.0 & 0.0 \\ 0.0 & 0.0 & 0.0 & -0.18 & -0.09 & -0.22 & 0.0 & 0.0 \\ 0.0 & 0.0 & 0.0 & 1.0 & 0.0 & 0.08 & 0.0 & 0.0 \\ 0.0 & 0.0 & 0.0 & 0.0 & 1.0 & 0.05 & 0.0 & 0.0 \end{bmatrix}$$

$$B = \begin{bmatrix} -0.12 & -1.2 & 0.65 & 0.75 \\ 0.46 & -0.15 & 0.08 & -0.73 \\ 0.0 & -0.04 & -5.8 & 0.35 \\ 0.95 & -0.02 & -0.1 & -0.38 \\ 0.01 & 0.26 & -0.02 & -0.03 \\ 0.05 & -0.01 & 0.08 & 0.33 \\ 0.0 & 0.0 & 0.0 & 0.0 \\ 0.0 & 0.0 & 0.0 & 0.0 \end{bmatrix}$$
**Flight Condition 21: 1 Knot. Main Rotor Speed = 30 rpm**

$$A = \begin{bmatrix} 0.0 & 0.0 & 0.01 & -0.95 & 1.8 & -0.33 & 0.0 & -32.0 \\ -0.01 & -0.05 & -0.01 & -1.2 & -0.64 & -1.1 & 32.0 & 0.13 \\ 0.04 & 0.0 & -0.28 & 0.03 & 1.3 & 1.8 & 1.6 & -2.5 \\ 0.03 & -0.03 & 0.0 & -3.8 & -1.3 & 0.04 & 0.0 & 0.0 \\ 0.01 & 0.0 & 0.0 & 0.17 & -0.7 & -0.09 & 0.0 & 0.0 \\ 0.0 & 0.0 & 0.0 & -0.21 & -0.03 & -0.23 & 0.0 & 0.0 \\ 0.0 & 0.0 & 0.0 & 1.0 & 0.0 & 0.08 & 0.0 & 0.0 \\ 0.0 & 0.0 & 0.0 & 0.0 & 1.0 & 0.05 & 0.0 & 0.0 \end{bmatrix}$$

$$B = \begin{bmatrix} -0.03 & -1.1 & 0.79 & 0.71 \\ 0.36 & -0.03 & 0.14 & -1.1 \\ 0.01 & 0.01 & -8.3 & 0.45 \\ 1.2 & 0.11 & -0.15 & -0.6 \\ 0.0 & 0.33 & -0.02 & -0.02 \\ 0.07 & 0.0 & 0.07 & 0.44 \\ 0.0 & 0.0 & 0.0 & 0.0 \\ 0.0 & 0.0 & 0.0 & 0.0 \end{bmatrix}$$

**Group III: Least Probable ( continued)****Flight Condition 22: 1 Knot. Weight = 20,000 lbs**

$$A = \begin{bmatrix} -0.02 & 0.0 & 0.01 & -1.0 & 2.4 & -0.54 & 0.0 & -32.0 \\ 0.01 & -0.05 & 0.0 & -2.2 & -0.66 & -1.0 & 32.0 & 0.17 \\ 0.02 & 0.0 & -0.22 & -0.1 & 1.4 & 2.1 & 1.6 & -3.3 \\ 0.02 & -0.03 & 0.0 & -2.4 & -0.91 & 0.03 & 0.0 & 0.0 \\ 0.0 & 0.0 & 0.0 & 0.2 & -0.61 & -0.08 & 0.0 & 0.0 \\ 0.0 & 0.0 & 0.0 & -0.13 & -0.08 & -0.24 & 0.0 & 0.0 \\ 0.0 & 0.0 & 0.0 & 1.0 & -0.01 & 0.1 & 0.0 & 0.0 \\ 0.0 & 0.0 & 0.0 & 0.0 & 1.0 & 0.05 & 0.0 & 0.0 \end{bmatrix}$$

$$B = \begin{bmatrix} -0.08 & -1.2 & 0.77 & 0.74 \\ 0.53 & -0.14 & 0.08 & -0.78 \\ 0.01 & -0.07 & -5.9 & 0.37 \\ 0.73 & -0.02 & -0.07 & -0.35 \\ 0.01 & 0.3 & -0.01 & -0.04 \\ 0.04 & -0.02 & 0.11 & 0.42 \\ 0.0 & 0.0 & 0.0 & 0.0 \\ 0.0 & 0.0 & 0.0 & 0.0 \end{bmatrix}$$
**Flight Condition 23: 45 Knots,  $\gamma = -7.06$  deg,  $\phi = 20$  deg. Weight = 20,000 lbs**

$$A = \begin{bmatrix} -0.05 & 0.27 & -0.23 & -0.88 & -6.9 & 7.4 & 0.0 & -32.0 \\ -0.27 & -0.08 & -0.01 & 7.5 & -0.91 & -74.0 & 25.0 & -0.71 \\ 0.07 & -0.01 & -0.41 & -6.2 & 76.0 & 2.1 & -20.0 & -0.86 \\ 0.0 & -0.03 & 0.02 & -2.6 & -0.77 & 0.39 & 0.0 & 0.0 \\ -0.01 & 0.01 & 0.0 & 0.36 & -0.87 & -0.16 & 0.0 & 0.0 \\ -0.01 & 0.01 & -0.01 & -0.37 & 0.09 & -0.64 & 0.0 & 0.0 \\ 0.0 & 0.0 & 0.0 & 1.0 & 0.02 & 0.03 & 0.0 & 0.35 \\ 0.0 & 0.0 & 0.0 & 0.0 & 0.77 & -0.63 & -0.35 & 0.0 \end{bmatrix}$$

$$B = \begin{bmatrix} -0.16 & -1.4 & 0.42 & 0.88 \\ 0.67 & -0.11 & 0.05 & -1.0 \\ 0.31 & -1.2 & -5.5 & 1.1 \\ 0.79 & 0.07 & 0.0 & -0.49 \\ 0.01 & 0.34 & 0.04 & -0.02 \\ 0.05 & 0.0 & 0.06 & 0.51 \\ 0.0 & 0.0 & 0.0 & 0.0 \\ 0.0 & 0.0 & 0.0 & 0.0 \end{bmatrix}$$
**Flight Condition 24: Hover. Forward CG**

$$A = \begin{bmatrix} -0.01 & -0.01 & 0.01 & -0.97 & 2.7 & -0.29 & 0.0 & -32.0 \\ 0.01 & -0.05 & 0.0 & -2.4 & -0.89 & -1.2 & 32.0 & 0.04 \\ 0.01 & 0.0 & -0.23 & 0.24 & 1.3 & 2.1 & 1.3 & -0.99 \\ 0.02 & -0.03 & 0.0 & -3.0 & -1.2 & 0.11 & 0.0 & 0.0 \\ 0.01 & 0.01 & 0.0 & 0.22 & -0.72 & -0.09 & 0.0 & 0.0 \\ 0.0 & 0.0 & 0.0 & -0.18 & -0.09 & -0.24 & 0.0 & 0.0 \\ 0.0 & 0.0 & 0.0 & 1.0 & 0.0 & 0.03 & 0.0 & 0.0 \\ 0.0 & 0.0 & 0.0 & 0.0 & 1.0 & 0.04 & 0.0 & 0.0 \end{bmatrix}$$

$$B = \begin{bmatrix} -0.1 & -1.2 & 0.41 & 0.73 \\ 0.53 & -0.12 & 0.03 & -0.76 \\ -0.02 & 0.01 & -5.9 & 0.32 \\ 0.9 & 0.01 & -0.11 & -0.33 \\ 0.01 & 0.3 & -0.06 & -0.04 \\ 0.06 & 0.02 & 0.08 & 0.37 \\ 0.0 & 0.0 & 0.0 & 0.0 \\ 0.0 & 0.0 & 0.0 & 0.0 \end{bmatrix}$$
**Flight Condition 25: 1 Knot. Aft CG**

$$A = \begin{bmatrix} -0.02 & 0.01 & 0.01 & -1.0 & 2.9 & -0.9 & 0.0 & -32.0 \\ 0.01 & -0.05 & -0.01 & -2.4 & -0.61 & -0.34 & 32.0 & 0.24 \\ 0.03 & 0.0 & -0.23 & 0.36 & 0.85 & 2.1 & 2.0 & -3.8 \\ 0.02 & -0.04 & 0.0 & -2.9 & -1.0 & -0.01 & 0.0 & 0.0 \\ 0.0 & 0.0 & 0.0 & 0.17 & -0.61 & -0.08 & 0.0 & 0.0 \\ 0.0 & 0.0 & 0.0 & -0.16 & -0.05 & -0.23 & 0.0 & 0.0 \\ 0.0 & 0.0 & 0.0 & 1.0 & -0.01 & 0.12 & 0.0 & -0.01 \\ 0.0 & 0.0 & 0.0 & 0.0 & 1.0 & 0.06 & 0.01 & 0.0 \end{bmatrix}$$

$$B = \begin{bmatrix} -0.08 & -1.2 & 0.87 & 0.74 \\ 0.51 & -0.17 & 0.12 & -0.77 \\ -0.01 & -0.02 & -5.9 & 0.35 \\ 0.88 & -0.02 & -0.08 & -0.4 \\ 0.01 & 0.3 & -0.01 & -0.03 \\ 0.05 & -0.02 & 0.1 & 0.41 \\ 0.0 & 0.0 & 0.0 & 0.0 \\ 0.0 & 0.0 & 0.0 & 0.0 \end{bmatrix}$$